HHS Public Access

Author manuscript

J Tissue Eng Regen Med. Author manuscript; available in PMC 2017 December 01.

Published in final edited form as:

J Tissue Eng Regen Med. 2016 December ; 10(12): 1041–1056. doi:10.1002/term.1889.

Nanoparticulate Delivery of Agents for Induced Elastogenesis in 3-Dimensional Collagenous Matrices

Lavanya Venkataraman[1,2,#], **Balakrishnan Sivaraman**[1,#], **Pratik Vaidya**[3], and **Anand Ramamurthi**[1,2,3,*]

[1]Department of Biomedical Engineering, Cleveland Clinic, Cleveland, OH 44195

[2]Department of Bioengineering, Clemson University, Clemson, SC 29634

[3]Department of Chemical and Biomedical Engineering, Cleveland State University, Cleveland, OH 44115

Abstract

The degradation of elastic matrix in the infrarenal aortic wall is a critical parameter underlying the formation and progression of abdominal aortic aneurysms (AAAs). It is mediated by the chronic overexpression of matrix metalloproteases (MMPs) -2 and -9, leading to a progressive loss of elasticity and weakening of the aortic wall. Delivery of therapeutic agents to inhibit MMPs, while concurrently coaxing cell-based regenerative repair of the elastic matrix represents a potential strategy for slowing or arresting AAA growth. Our prior studies have demonstrated elastogenic induction of healthy and aneurysmal aortic smooth muscle cells (SMCs) and inhibition of MMPs, following exogenous delivery of elastogenic factors such as TGF-β1, as well as MMP-inhibitors such as doxycycline (DOX) in two-dimensional (2-D) culture. Based on these findings, and others that demonstrated elastogenic benefits of nanoparticulate delivery of these agents in 2-D culture, we have developed poly(lactide-co-glycolide) nanoparticles for localized, controlled and sustained delivery of DOX and TGF-β1 to human aortic SMCs (HASMCs) within a three-dimensional (3-D) gels of type-I collagen gel, which closely evoke the arterial tissue microenvironment. DOX and TGF-β1 released from these NPs influenced elastogenic outcomes positively within the collagen constructs over 21 days of culture, which were comparable to that induced by exogenous supplementation of DOX and TGF-β1 within the culture medium. However, this was accomplished at doses ~20-fold lower than the exogenous dosages of the agents, illustrating that their localized, controlled, and sustained delivery from NPs embedded within a 3-D scaffold is an efficient strategy for directed elastogenesis.

1. Introduction

Progression of abdominal aortic aneurysm (AAA) disease, characterized by gradual aortic wall thinning, weakening, leading to ultimate rupture, appears to be related to two factors, namely, (a) chronically high levels of matrix protease activity, primarily that of the

*To whom correspondence should be addressed (ramamua@ccf.org, phone: 216-444-4326, fax: 216-444-9198).

#Equal contributions

Conflicts of Interest: No conflicts of interest exist

elastolytic MMPs -2 and -9, which are incited by inflammatory cells recruited to the site of aortic tissue injury (Blanchard 1999; Daugherty and Cassis 2002; Annambhotla et al., 2008), and (b) the inability of vascular parenchymal cells to preserve and restore disrupted vascular wall matrix, especially the elastic matrix component (Chadwick et al., 1995; Li et al., 1998; Patel et al., 2006). In prior work conducted in our lab, we have shown that cultured adult vascular smooth muscle cells (SMCs) can be stimulated to enhance *de novo* elastin synthesis and elastic matrix assembly using biomolecular 'elastogenic' factors (EFs) such as transforming growth factor-β1 (TGF-β1) and hyaluronan oligomers (Kothapalli et al., 2009; Kothapalli et al., 2009; Venkataraman and Ramamurthi 2011). Differently, studies in both animal models (Curci et al., 1998; Manning et al., 2003; Bartoli et al., 2006) and humans (Curci et al., 2000; Baxter et al., 2002; Prall et al., 2002) have shown MMP inhibitors such as doxycycline (DOX) to slow AAA growth, in part by attenuating elastolytic activity in the AAA wall tissue. Further, pilot studies conducted on two-dimensional (2-D) cell cultures in our laboratory, suggest that DOX enhances or inhibits elastic matrix synthesis itself depending on its dose. To minimize the amounts of active agents delivered to the AAA tissue, and avoid adverse side-effects associated with systemic DOX delivery (Baxter et al., 2002; Bendeck et al., 2002), it is important to evaluate strategies for localized, controlled, and sustained delivery at AAA sites. This would be beneficial towards stimulating regenerative repair of elastic matrix at the AAA site and in parallel, inhibiting matrix proteolysis towards improving quality and quantity of such matrix regeneration.

Localized and controlled delivery of the EFs described above is crucial, since we have shown their effects to be highly dose-dependent (Gacchina et al., 2011; Gacchina et al., 2011). For example, the regulatory effects of growth factors like TGF-β1 are critically dependent on controlling delivery dose since the growth factors is known to have biphasic effects that depend on its concentration (Battegay et al., 1990). While TGF-β1 provided at concentrations of less than 10 ng/mL, have been shown to suppress cell proliferation and improve synthesis and assembly of elastin and elastic matrix components (Stegemann and Nerem 2003; Kothapalli et al., 2009), at higher concentrations it has been shown to induce the switch of SMCs to an osteogenic phenotype and promote matrix mineralization (Simionescu et al., 2005). Recent studies have also shown that when DOX is delivered locally to AAA tissues using mini-osmotic pumps or peri-aortic foams, the doses necessary to attenuate MMP activity are nearly 100 fold lower than that required when systemically delivered (Bartoli et al., 2006; Yamawaki-Ogata et al., 2010). Moreover, systemic inhibition of MMPs is undesirable since MMPs participate in matrix remodeling and turnover in healthy tissues (Galis and Khatri 2002). Localized DOX delivery for AAA therapy thus has the potential to overcome several undesirable side effects associated with its systemic delivery (Baxter et al., 2002; Bendeck et al., 2002).

In a recent study we have shown that controlled and sustained delivery of DOX from polymeric nanoparticles (NPs) is feasible and that the released DOX maintains its functional effects on cultured cells (Sivaraman and Ramamurthi 2013). In the current study, we utilize an *in vitro* model of dynamically conditioned, cell-compacted tubular collagen gel conduits that mimic the three-dimensional (3-D) aortic tissue microenvironment, to assess the elastogenic inductive effects of TGF-β1 and the anti-elastolytic effects of DOX, again delivered from NPs, on healthy human aortic SMCs, compared to their effects when

exogenously delivered. The study seeks to demonstrate the efficacy of NP-delivered EFs and elastolysis inhibitors in augmenting *de novo* elastic matrix deposition within a 3-D, collagenous tissue microenvironment which is known to switch SMCs to a quiescent phenotype and suppress elastin synthesis by cells (L'Heureux et al., 1993; Kim et al., 1999; Song et al., 2000), and any possible benefits of this particular mode of active agent delivery over to their exogenous supplementation to the culture medium.

2. Materials and Methods

2.1. Formulation of agent-loaded PLGA NPs

A double emulsion solvent evaporation method was used to synthesize agent-loaded NPs (Guzman et al., 1996; Song et al., 1997), with poly(vinyl) alcohol (PVA; Sigma-Aldrich, St. Louis, MO) as the stabilizer. PVA is widely used as a stabilizer in the formulation of PLGA NPs, and has been shown to impart them with a negative surface charge or zeta potential (ζ potential = - 28 mV) (Labhasetwar et al., 1998; Sivaraman and Ramamurthi 2013; Sylvester et al.,). Briefly, poly (*dl*-lactic-co-glycolic acid) (PLGA; 50:50 lactide: glycolide; inherent viscosity = 0.95-1.20 dL/g in hexafluoroisopropanol; Durect Corporation, Birmingham, AL) was dissolved in dichloromethane (Sigma-Aldrich) at a concentration of 2.5-3.0 % w/v. Recombinant human TGF-β1 (R&D Systems, Inc., Minneapolis, MN) was reconstituted as per specifications listed by the company in sterile 4 mM HCl containing 0.1% w/v bovine serum albumin (BSA; Amresco, Inc. Solon, OH), divided into single-use aliquots and stored at -80 °C prior to encapsulation. During the encapsulation process, an aliquot of TGF-β1 (50 μL) was mixed with an equal volume of an aqueous solution of 1% w/v BSA (Davda and Labhasetwar 2005), and added to the PLGA solution at loading concentrations of 1000, 2000 ng and 5000 ng of TGF-β1. This solution was sonicated for 1 min on ice using a probe sonicator (Q500; QSonica LLC, Newtown, CT) at an amplitude of 20% to create a water-in-oil emulsion. This primary emulsion was then added to an aqueous solution of 0.25% w/v PVA and sonicated for 1 min to create the final water-in-oil-in-water emulsion. The resulting emulsion was stirred for 16 h at room temperature, following which it was desiccated for 1 h under vacuum to remove any residual traces of organic solvent used. The NP suspension formed was centrifuged at 35,000 rpm in a Beckman L-80 ultracentrifuge (Beckman Instruments, Inc., Palo Alto, CA) to recover the NPs. The NPs were washed and ultracentrifuged twice at 30,000 rpm to remove traces of surfactants and unencapsulated TGF-β1, and finally lyophilized for 48 h. The supernatant solutions from the centrifugation steps during the NP formulation process were stored for subsequent analysis and quantification of unencapsulated TGF-β1 (see section 2.2).

DOX (doxycycline hyclate; Sigma-Aldrich) was encapsulated within NPs via the same protocol listed above, at two different loading percentages (2% w/w and 5% w/w ratios of DOX to PLGA), using 0.25% w/v PVA as the stabilizer during the formulation. Tetracyclines are known to be sensitive to light (Davies et al., 1985; Honnorat-Benabbou et al., 2001), and hence, appropriate precautions were taken to ensure minimal exposure to light during the formulation and release process.

2.2. Efficiency of TGF-β1 and DOX encapsulation within NPs

The supernatant fractions generated during the NP formulation process were assayed to quantify the unencapsulated TGF-β1 or DOX. The total amount of TGF-β1 in the supernatant was quantified using a Quantikine® enzyme-linked immunosorbent assay (ELISA) kit specific for human TGF-β1 (R&D Systems, Inc.) (Jhunjhunwala et al., 2012). The supernatant containing unencapsulated DOX was analyzed via UV spectrophotometry (SpectraMax M2, Molecular Devices, Inc., Sunnyvale, CA) using the absorbance peak exhibited by DOX at 270 nm (Injac et al., 2007; Mitic et al., 2008). The height of this peak was calibrated to serial dilutions of a 1.0 mg/mL DOX solution to obtain a standard curve, which was used for quantifying the amount of unencapsulated DOX in the supernatant. The total amount of TGF-β1 or DOX encapsulated in the NPs and the overall encapsulation efficiencies were determined by subtracting the total amount of unencapsulated TGF-β1 or DOX from their respective total amounts, added during NP formulation. The supernatant from control formulations (blank NPs containing no active agent) were also analyzed to eliminate possible absorbance contributions due to PLGA or PLGA breakdown products from these samples.

2.3. Size and surface charge measurements on TGF-β1 and DOX-loaded PLGA NPs

Dynamic light scattering (DLS) was used to determine the mean hydrodynamic diameters of formulated NPs and assess the overall homogeneity of their hydrodynamic sizes. NP surface charge or ζ-potential was quantified via a phase analysis light scattering technique. Both measurements were carried out using a commercial particle-sizing system (PSS/NICOMP 380/ZLS, Particle Sizing Systems, Santa Barbara, CA), as described previously (Sivaraman and Ramamurthi 2013).

2.4. Characterizing DOX and TGF-β1 release from PLGA NPs in vitro

DOX and TGF-β1 release from NPs was carried out over 21 days at 37 °C on a shaker at 100 rpm, in phosphate buffer saline (PBS, pH 7.4; Sigma-Aldrich) and PBS containing 0.1% w/v BSA, respectively. BSA was added to the release media, in order to minimize any potential non-specific growth factor binding to the walls of the tube/cell chamber into which TGF-β1 was released (Davda and Labhasetwar 2005; Tan et al., 2011). Briefly, 1.5 mL polypropylene microcentrifuge tubes ($n = 3$ per formulation) were filled with 1.0 mL of NP suspensions containing 10.0 mg/mL of TGF-β1 loaded NPs (1000, 2000 and 5000 ng of TGF-β1) and 0.2 and 0.5 mg/mL of DOX-loaded NPs (2% and 5% w/w DOX to PLGA). At each time point for analysis, the samples were centrifuged (7000 rpm, 20 min for TGF-β1 NPs; 10,000 rpm, 30 min for DOX NPs) at 4 °C in a microcentrifuge (Beckman Microfuge 16®, Beckman Coulter, Inc.), the supernatants withdrawn to quantify TGF-β1 or DOX content, and volume-replenished with the corresponding fresh buffer. The supernatant solutions from TGF-β1 release were frozen at -20 °C until further analysis, while that from the DOX release were analyzed immediately to quantify DOX released.

TGF-β1 and DOX released were quantified using ELISA and UV-spectrophotometry respectively, as described above in Section 2.2. The DOX standards for the calibration curve used to estimate its release were incubated under the same conditions as the NP samples, to

avoid any potential effects arising due to time- and temperature-dependent DOX degradation (Haerdi-Landerer et al., 2008; Sunaric et al., 2009).

2.5. Determining in vitro cytotoxicity of TGF-β1 and DOX-loaded PLGA NPs

The potential cytotoxicity of TGF-β1 and DOX loaded PLGA NPs on cultured human aortic SMCs (HASMCs) was assessed using a LIVE/DEAD® cell viability assay (Invitrogen, Carlsbad, CA). Briefly, HASMCs (Passage 5; Cell Applications, San Diego, CA) were seeded at a density of 8×10^4 cells/well in a sterile, 12-well plate (Beckton Dickinson, Franklin Lakes, NJ) and allowed to adhere over a 14 day period in DMEM-F12 cell culture media (Invitrogen, Carlsbad, CA) supplemented with 20% v/v fetal bovine serum (FBS; PAA Laboratories, Etobicoke, Ontario) and 1% v/v penicillin–streptomycin (PenStrep; Thermo Fisher, South Logan, UT). The TGF-β1 (2000 ng loading) and DOX-loaded PLGA NPs (5% w/w loading) were added at concentrations of 0.1, 0.2 and 0.5 mg/mL to the cultures, and incubated for 24 h prior to assessing their viability. Additionally, we also tested a combination of 0.3 mg/mL of TGF-β1 loaded NPs (loaded with 2000 ng TGF-β1) and 0.2 mg/mL of 5% DOX loaded NPs. Blank PLGA NPs containing no encapsulated active agent were tested as an active agent control, while NP- untreated cultures served as the treatment controls. Stained cells were viewed using an Olympus IX51 fluorescence microscope (Olympus America, Center Valley, PA). Six different regions were assessed for each replicate culture.

2.6. Experimental design: Nanoparticulate delivery of agents

The goal of this study was to compare if localized, nanoparticulate delivery of DOX and TGF-β1 (hereto collectively referred to as '*agents*') provides benefits over their exogenous delivery to quantity and quality of elastogenesis by adult vascular SMCs in a 3-D collagenous tissue microenvironment. Cellularized collagen gels were cultured under three experimental conditions, namely, with blank NPs (BNP) and agent-loaded NPs (ANP) embedded within the collagen constructs, and with exogenous agents (DOX, TGF-β1) delivered in the culture medium to the constructs (Control; EDC) at concentrations equivalent to that achieved at steady-state or near-steady-state delivery from the NPs, as determined from their release curves. The details on the exact doses of BNP, ANP and EDC used within the collagen constructs to evaluate their functional effects or benefits towards the elastogenic induction of HASMCs are provided in Section 2.8 (below). Continuous cyclic stretch was provided to the constructs in all three cases at 2.5% strain and 1.5 Hz frequency, since these dynamic stretch parameters were shown by our lab previously to enhance matrix deposition and align cells and increasingly deposited matrix (unpublished data). The constructs were cultured for 21 days, at the end of which quantity and quality of elastic matrix, cell density and phenotype, and MMP content and activity were analyzed.

2.7. Bioreactor for Dynamic Stimulation of Constructs

A bioreactor capable of providing cyclic, circumferential stretch to tubular collagen gel constructs was developed. As shown in Figure 1, the bioreactor consists of a cylindrical culture chamber, with centrally placed silicone tubing, around which the collagen gel constructs compacted. The silicone tubing was in turn connected to metallic bellows (Mini-Flex, Ventura, CA), forming a closed, airtight conduit into which a constant volume of water

was maintained. The bioreactor therefore worked on the principle that when the bellows contract and expand, the resultant displacement of water within the closed loop will proportionally expand or contract the silicone tube, and in turn the cell-seeded collagen gel construct around it. The contraction and expansion of the bellows were controlled by a stepper motor (All Motion, Union City, CA) and its motor controller, programmed to deliver the required 2.5 % strain at 1.5 Hz frequency.

2.8. Formulation of NP-loaded Collagen Constructs

The collagen constructs were formulated as detailed in a previous paper (Venkataraman and Ramamurthi 2011). Briefly, acid-solubilized rat-tail type-I collagen (BD Biosciences, Bedford, MA) was mixed with 5× DMEM-F12 and 0.1N NaOH and added drop wise to titrate the solution to pH 7.4. Following this, the NPs were added at a final concentration of 0.5 mg/mL, (i.e., 0.2 mg/mL of NPs loaded with DOX at 5% w/w and 0.3 mg/mL of NPs loaded with 2000 ng of TGF-β1; **ANPs**). This overall concentration was decided upon based on the outcomes of our studies on release kinetics of the agents from NPs in PBS and of their cytotoxicity studies, to be explained in the discussion section. For constructs cultured with blank NPs (BNPs), the agent-free NPs at a concentration of 0.5 mg/mL was used. HASMCs (5×10^5/mL) were then added to this viscous mixture, mixed well by gentle pipetting, and then added to the culture chambers of the bioreactors. The constructs were cultured in DMEM-F12 medium containing 10 % v/v fetal bovine serum (FBS) and 1% v/v penicillin-streptomycin (PS). In cultures designated as exogenous delivery controls (EDC), DOX and TGF-β1 were exogenously supplemented to the medium at concentrations equivalent to steady-state levels released from the respective NPs over the 21 day culture period, as determined from the DOX/TGF-β1 release curves (see Section 2.4). Since the concentration of TGF-β1-releasing NPs within the constructs was much lower (0.3 mg/mL) than that (10 mg/mL) used in the TGF-β1 release studies, it was necessary to apply a correction to the steady-state doses obtained from the release curve (corresponding to 10 mg/mL of NPs) to ascertain the equivalent exogenous dose. Thus, the exogenous doses of DOX and TGF-β1 were 11.2 μg/mL for DOX and 0.20 ng/mL for TGF-β1, respectively. For these constructs, the culture medium was again replaced every 2 days, and supplemented with new DOX and TGF-β1 at each of the medium change events. All constructs were harvested 21 days after seeding, rinsed 3 times in sterile PBS, and processed for various biochemical assays.

2.9. Compaction of Tissue Constructs

All constructs were photographed at regular intervals, using a digital camera, and their lengths and central widths were measured using the ImageJ imaging software (NIH, Bethesda, MD). At least five measurements for central width and three measurements for the length were made per construct. The extent of compaction of constructs was calculated and represented as the aspect ratio of length to outer diameter (O.D.) at harvest on day 21.

2.10. DNA Assay for Cell Quantification

After 21 days of culture, the collagen constructs were rinsed with PBS, flash-frozen, lyophilized and digested in 5 mg/mL proteinase-K (Life Technologies, Carlsbad, CA) at

65 °C for 10 hours. After inactivating the enzyme at > 75 °C, the samples were then centrifuged at 14,000 rpm to pellet any possible NPs. The supernatants were sonicated and a Hoechst 33258 dye (Life Technologies, Carlsbad, CA) -based fluorometric DNA assay was performed to calculate the DNA content (Labarca and Paigen 1980). Cell numbers were calculated based on an estimate of 6 pg DNA/cell, and normalized to mg tissue weights for comparison, (n = 5/case).

2.11. RT-PCR for mRNA Expression of SMC Phenotypic Markers and Matrix Proteins

Harvested constructs were rinsed in sterile PBS, cut into small (1–2 mm long) pieces and stored in RNAlater (Qiagen, Valencia, CA) solution until processing, and RNA isolated using an RNeasy kit (Qiagen, Valencia, CA), according to the manufacturer's instructions. RNA content was measured using a Ribo-green assay kit (Life Technologies, Carlsbad, CA), and 250 ng total RNA was reverse transcribed into cDNA, using iScript cDNA synthesis kit (Biorad, Hercules, CA). RT-PCR was performed for SMC markers such as smooth muscle actin-α (*SMA*), caldesmon *(CALD1)* and osteopontin *(OPN),* elastic matrix proteins such as elastin *(ELN),* fibrillin-1 *(FBN1),* fibulin-5 *(FBLN5),* lysyl oxidase *(LOX)* and collagen 1 (*COL1A1*), and MMPs -2 *(MMP2)* and -9 *(MMP9)*. Gene expressions were estimated (duplicate readings, n = 5 per sample) using the comparative threshold method with 18s as the normalizing gene (Livak and Schmittgen 2001). Primers for all genes were either purchased as optimized primer sets from Real Time Primers (Elkins Park, PA), or designed using the NIH software PerlPrimer® (Marshall 2004) and purchased from Applied Biosystems (Foster City, CA; Table 1).

2.12. Fastin Assay for Elastin Content

Matrix elastin quantified contained both less crosslinked alkali-soluble elastin, and the highly crosslinked alkali-insoluble elastin. Lyophilized construct segments were digested in 0.1 N NaOH to solubilize alkali-soluble matrix elastin, followed by in 0.25 M oxalic acid to obtain solubilized alkali-insoluble matrix elastin, as described previously (Venkataraman and Ramamurthi 2011). Digested samples were once again centrifuged at 14000 rpm for 30 minutes to eliminate any possible contamination from NPs. Elastic matrix in both the digested aliquots were quantified using the Fastin assay kit (Accurate Scientific and Chemical Corporation, Westbury, NY), as per the manufacturer's instructions and added to obtain the total generated amounts of elastic matrix.

2.13. Western Blotting for Elastic Matrix Assembly Proteins

Western blotting was performed to broadly assess if phenotypic marker proteins expressed by HASMCs (n = 1 construct/treatment condition) such as α-smooth muscle actin (SM-α; an early-stage marker), mid-stage markers such as smooth muscle-22-α (SM22), calponin and caldesmon, and myosin heavy chain (MHC; a late-stage marker) were altered by exposure to the NPs, or agents. Western blots were also performed to assess treatment-specific changes to synthesis of elastic matrix assembly proteins (n = 3 constructs/treatment condition) such as LOX, fibrillin-1 and fibulin-5, and elastolytic matrix metalloproteases MMPs-2 and -9 (n = 3 constructs/treatment condition).

Lyophilized segments of constructs were added to RIPA lysis buffer (Life Technologies, Carlsbad, CA) with a protease inhibitor cocktail (Thermo Scientific, Rockford, IL) and homogenized to solubilize proteins. A bicinchonic acid (BCA) assay (Thermo Scientific, Rockford, IL) was performed to measure concentration of total protein in all samples. Samples containing 10 μg of protein were loaded into lanes of SDS-PAGE gels (Life Technologies), along with a BenchMark™ pre-stained molecular weight ladder (Invitrogen). Following the separation of proteins based on their molecular weights, the protein bands on the gel were transferred dry onto a nitrocellulose membrane using an iBlot transfer system (Life Technologies) according to the manufacturer's instructions.

All blots were blocked with Odyssey Blocking Buffer (LI-COR Biosciences, Lincoln, NE) for 1 h, following which they were immunolabeled with primary antibodies for 16 h at 4 °C, with a mouse monoclonal antibody against β-actin (Sigma–Aldrich) as the loading control. All primary antibodies were purchased from Abcam (Cambridge, MA), except LOX, fibrillin-1 and fibulin-5 (Santa Cruz Biotechnology, Inc., Dallas, TX), and MMP-9 (Millipore, Billerica, MA). Labeling with secondary antibodies was carried out using IRDye® 680LT goat-anti-rabbit (1:15,000 dilution) and IRDye® 800CW goat anti-mouse (1:20,000 dilution) polyclonal antibodies (LI-COR Biosciences) for 1 h at room temperature. A LI-COR Odyssey laser-based scanning system was utilized for fluoroluminescence detection of the protein bands. The band intensities of the protein of interest calculated in relative density units (RDU) using the ImageJ software, were first normalized to that of their respective β-actin bands (loading control) to enable comparisons between the different test cases in the same blot. These normalized band intensities were further normalized to those of the exogenous agent delivery condition (EDC) to evaluate the fold-change in expression of the different proteins and MMPs. The results presented in this manuscript were averaged from three replicate gels run per culture treatment.

2.14. Gelatin Zymography for Detection of Enzyme Activities of MMPs -2 and -9

Gelatin zymography was performed to semi-quantitatively estimate differences the enzyme activities of the MMPs -2 and -9, between the treatment conditions (n = 3/treatment condition), as described earlier (Venkataraman and Ramamurthi 2011). Protein samples (10 μg) homogenized in RIPA buffer (as discussed in Section 2.13) were loaded into each lane of a 10 % zymogram gel (Invitrogen). Enzyme activity was represented as a fold change in RDU values relative to EDC constructs (control).

2.15. Visualization of Elastic Matrix

Tissue constructs harvested after 21 days of treatment were rinsed in PBS, and 0.5-cm-long sections fixed in 4% w/v paraformaldehyde, dehydrated and embedded in paraffin wax. Histology was performed on 30 μm-thick cross- and longitudinal- sections using an elastic stain kit (ScyTek Laboratories Inc., Logan, UT) to visualize the ultrastructure of elastic matrix content in the constructs. Immunofluorescence (IF) was performed on 10 μm cross- and longitudinal- sections, using rabbit anti-rat primary antibodies against elastin (Millipore) and fibrillin-1 (Abcam) and Alexa633-conjugated IgG secondary antibodies (Invitrogen). The labeled sections were mounted in Vectashield with 4′,6-diamidino-2-phenyindole (DAPI; Vector Laboratories, Inc. Burlingame, CA), which labels the nuclei of cells. Imaging

was carried out using an Olympus IX51 fluorescence microscope (Olympus America, Center Valley, PA). Six different regions were assessed per treatment condition to evaluate outcomes.

2.16. Statistical Analysis

All experiments were performed on n = 5 biological replicates per treatment condition, unless mentioned otherwise. Histology and IF were performed on segments from n = 1 construct per condition. All quantitative and semi-quantitative results are represented as mean ± standard deviation per condition. Conditions were deemed to be significantly different for p values ≤ 0.05 calculated using one-way ANOVA.

3. Results

3.1. Formulation and characterization of agent-loaded PLGA NPs

The mean hydrodynamic diameters of the blank (agent-free), TGF-β1- and DOX-loaded PLGA NPs were comparable (~300-350 nm), as listed in Table 1. The surface charge (ζ-potential) on these NPs ranged between -26 and -32 mV (Tables 1 and 2), values comparable to that obtained in our previous studies that also generated PVA-functionalized NPs (-28 mV) (Sivaraman and Ramamurthi 2013; Sylvester et al.,). Encapsulation of TGF-β1 or DOX within the PLGA NPs did not alter their size or surface charge significantly.

The efficiency of encapsulating TGF-β1 within NPs was determined to be 84.0 ± 9.0%, as calculated from values measured for NP preparations for the different TGF-β1 loadings (total of n = 6 replicates/loading; Table 2), while the overall encapsulation efficiency of DOX was 58.4 ± 0.7 % (total of n = 6 replicates/loading; Table 2). In the case of both the agents, encapsulation efficiency was not impacted by the % w/w loading of the agent in any statistically significant manner.

3.2. *In vitro* release of TGF-β1 and DOX from PLGA NPs

The *in vitro* release profiles for TGF-β1 and DOX from the PLGA NPs are shown in Figure 2. Release studies for TGF-β1 loaded NPs was carried out at a NP concentration of 10 mg/mL, as has been done in previous studies by other groups (Lu et al., 2000; Lu et al., 2001), so as to obtain levels of released TGF-β1 that could be detected reliably via ELISA. As observed in Figure 2, TGF-β1 release from the PLGA NPs was characterized by a rapid burst phase initially over the first 24 h, followed by a more gradual release profile that attained a plateau by day 7 (corresponding to a steady state concentration of ~2.0 ng/mL for 1000 ng of loaded TGF-β1, ~6.5 ng/mL for 2000 ng of loaded TGF-β1, and 4.2 ng/mL for 5000 ng of loaded TGF-β1).

The DOX-loaded NPs also demonstrated an initial burst release of DOX over the first 24 h, which was followed by a slower exponential release phase over several days. The levels of DOX released from the NPs ranged between 8.2 – 15.4 μg/mL at day 21, and the release did not plateau even after 60 days (Supplementary Figure 1).

3.3. Effects of NPs and active agents on construct compaction and cell proliferation

After 21 days, constructs under all treatment conditions actively compacted and were found to have an ultimate length: O.D. aspect ratio ranging between 8.4 and 9.5 (Supplementary Figure 2), although no significant differences were observed in the extent of compaction between the different treatment conditions ($p = 0.91$ for both sets of NP-treated constructs, with and without factors, compared to EDC).

At all tested NP doses (0.1, 0.2, and 0.5 mg/mL), standalone TGF-β1-loaded NPs (2000 ng loading) and DOX-NPs (5% w/w loading) did not impact viability of HASMCs in 2-D culture, similar to BNPs delivered at the same doses. Likewise, the combination of these two NP types (0.2 mg/mL of DOX-NPs and 0.3 mg/mL of TGF-β1-NPs) had no adverse effects on HASMC viability (Supplementary Figure 3). Average viable cell counts measured within the collagen constructs at 1 day post-seeding were $(1.5 \pm 0.25) \times 10^5$ cells/mg of tissue. Cell counts at 21 days were comparable to that at seeding with no significant differences between treatments (Figure 3; $p = 0.93$ for BNP vs. EDC, $p = 0.22$ for ANP vs. EDC, and $p = 0.34$ for BNP vs. ANP).

3.4. NP and active agent effects on SMC phenotype

Detailed outcomes of the phenotypic characterization of the HASMCs utilized in these studies have been described in an earlier publication by our group (Gacchina et al., 2011). RT-PCR was performed to evaluate the mRNA expressions of SMC phenotypic markers following culture within the collagen constructs with ANPs or BNPs and EDC, in our bioreactor system. Expression of α-SMA and caldesmon, both contractile SMC markers, was maintained upon culture with NPs compared to EDC ($p = 0.97$ (SMA) and 0.99 (caldesmon) for BNP vs. EDC and $p = 0.93$ (SMA) and 0.99 (caldesmon) for ANP vs. EDC), as seen in Figure 4. Gene expression of osteopontin, a marker for synthetic/activated SMC phenotype in presence of BNPs or ANPs was also not statistically different from EDC ($p = 0.08$ for BNP vs. EDC, and 0.07 for ANP vs. EDC; Figure 4). There were no statistical differences in gene expression for any of the tested markers between cultures with BNPs and ANPs ($p = 0.97$, 0.9, and 0.88 for SMA, caldesmon, and osteopontin respectively). Consistent with gene expression data, western blots (Supplementary Figure 4A) also showed no apparent differences in synthesis of the SMC marker proteins α-SMA, calponin, caldesmon, SM22α and MHC by cells cultured with both exogenous agents and NPs.

3.5. Effects of NPs and active agent release on elastic matrix synthesis and assembly

RT-PCR was used to analyze the treatment-specific differences in the cellular expression of genes coding for proteins involved in elastic matrix assembly, namely, *ELN, FBN1, FBLN5* and *LOX* (Figure 5A). When compared to EDC constructs, *ELN* expression was 3.0 ± 0.1 -fold lower ($p < 0.001$) in BNP constructs. *ELN* expression within the ANP-treated constructs was similar to that in EDC constructs ($p = 0.512$) and significantly higher (2.5 ± 0.5 fold; $p = 0.002$) than in the BNP constructs. Similar trends were observed for *FBN1* and *FBLN5,* with their expression in ANP-treated constructs being 3.1 ± 0.9-fold and 3.6 ± 1.2-fold higher respectively, versus BNP-treated constructs ($p < 0.05$ in both cases). Constructs cultured with ANPs showed similar expression levels of *FBLN5* ($p = 0.99$) as EDC constructs, but significantly lower expression of *FBN1* (1.5 ± 0.1 -fold; $p < 0.001$

compared to EDC constructs). Expression of *LOX* on the other hand, was higher in constructs cultured with BNPs (1.5 ± 0.3 –fold increase; $p = 0.012$) and ANPs (1.7 ± 0.5 -fold increase; $p = 0.041$) compared to EDC constructs. mRNA expression for *COL1A1* in constructs cultured with BNPs and ANPs was not significantly different compared to that in EDC constructs ($p = 0.07$ for BNP constructs and 0.12 for ANP constructs vs. EDC constructs). Again there was no significant difference in *COL1A1* expression between BNP and ANP-treated constructs.

A Fastin assay quantified the amount of elastic matrix generated by HASMCs within the differently-treated groups of constructs (Figure 5B). Total elastic matrix amounts generated within ANP constructs (20.7 ± 1.8 μg/mg) were similar to that in EDC (21.3 ± 2.0 μg/mg, $p = 0.62$), while that in BNP constructs were significantly lower than that in both EDC and ANP constructs (10.1 ± 2.6 μg/mg, $p < 0.001$ vs. both EDC and ANP constructs).

Western blotting was performed to semi-quantitatively estimate the cellular production of LOX, fibrillin-1 and fibulin-5. β-actin normalized intensities of bands corresponding to active LOX protein were higher in the constructs treated with NPs, both BNPs and ANPs, compared to EDC (Supplementary Figure 4B). However, in the other replicate blots, the band intensities for EDC-treated constructs were too low to be reliably quantified. Therefore statistical comparison representing differences in LOX protein content have not been performed. At the 10 μg protein concentrations tested, the amounts of fibrillin-1 and fibulin-5 were too low to be detected on western blots (data not shown).

3.6. MMPs -2 and -9-Mediated Elastolysis

As seen in Figure 6A, RT-PCR analysis showed *MMP2* expression to be significantly enhanced upon culture of constructs with NPs. Constructs with BNPs showed an average of 4.2 ± 0.6 -fold increase in *MMP2* expression over that in EDC constructs ($p < 0.001$). The release of active agents from the NPs lowered *MMP2* expression 1.8 ± 0.3-fold compared to that in constructs cultured with BNPs ($p < 0.001$), though expression levels were still significantly higher than in EDC constructs (2.4 ± 0.3 -fold; $p < 0.001$). Expression of *MMP9* in constructs treated with BNPs and ANPs was not different relative to the EDC constructs ($p = 0.06$ for BNP constructs, and 0.18 for ANP constructs vs. EDC constructs). *MMP2* expression was in general much higher than that of *MMP9* ($C_t = 20.4 \pm 0.9$ for *MMP2*, $C_t = 36.5 \pm 0.4$ for *MMP9; n* = 14).

Western blotting estimated differences in MMP protein synthesis within the constructs subjected to the different treatments. As seen in Figures 6B and C, the intensity of the 72 kDa bands corresponding to the zymogen form of MMP-2 were lower in BNP constructs compared to EDC constructs (3.0 ± 0.9 –times lower compared to EDC constructs, $p = 0.03$) while there were no differences between the ANP and EDC constructs ($p = 0.1$). Differences in the band intensities for MMP-2 zymogen between BNP and ANP constructs were insignificant ($p = 0.19$). In contrast, the intensities of the 66 kDa bands corresponding to active MMP–2 were found to be higher in both sets of NP-treated constructs (1.7 ± 0.4 fold and 1.5 ± 0.4-fold increase over EDC constructs; $p = 0.05$ and 0.27, respectively).

While the 92 kDa MMP-9 zymogen band was undetectable in all cultures, the intensities of the β-actin-normalized 82 kDa band corresponding to active MMP-9 enzyme were found to be significantly decreased to similar extents in both ANP- and BNP-treated constructs compared to EDC constructs (0.22 ± 0.17 & 0.20 ± 0.14 times amounts in EDC constructs respectively, $p = 0.001$ in both cases; Figure 6C).

Zymography was performed to estimate and compare the activity of the gelatinases present within the different groups of constructs (Figures 6D and E). Activities of the MMP-2 zymogen and active MMP-2 enzyme within the ANP constructs were 2.1 ± 0.7-fold and 1.9 ± 0.6- fold higher than in the EDC constructs ($p = 0.2$ and $p = 0.01$ vs. EDC constructs) but lower than in the BNP constructs (0.75 ± 0.24-fold and 0.54 ± 0.17-fold respectively for zymogen and active forms, $p = 0.37$ and 0.023) On the other hand, at the protein concentrations assayed, bands corresponding to active MMP–9 enzyme were detected only in EDC constructs. They were not detected in either of the NP-treated constructs in any of the 3 biological replicates tested. Zymogen bands of MMP-9 enzyme were again undetected in all three conditions.

3.7. Matrix Ultrastructure

As seen in Figures 7 (Elastic Stain) and 8 (immunofluorescence labeling for elastin), cells and elastic matrix fibers deposited within the constructs were predominantly oriented along their long axis under all treatment conditions, although circumferential orientation of the matrix was observed in the regions closer to the lumen of the tubular constructs. As in histological sections, in immunofluorescence micrographs, elastic fibers were apparent and mostly oriented along the long axis of the constructs, except close to the lumen.

4. Discussion

In our pilot studies, we determined that the treatment of adult vascular SMCs within collagen constructs with elastogenic factors (such as TGF-β1) and DOX improve outcomes of induced elastogenesis. While these studies mimic an *in vivo* tissue microenvironment, these elastogenic factors and DOX were supplemented exogenously to the culture media. There are two limitations to such delivery. First, this mode of delivery of the active agents cannot be translated for *in vivo* induced regenerative matrix repair at sites of tissue proteolysis. Second, even in delivering these agents to cells within tissue constructs *in vitro,* there are likely to be limitations to their diffusion into the tissue constructs, resulting in reduced effects/benefits to the cells in the interior of the tissue constructs. Thus, in the context of consistent *in situ* matrix preservation, regeneration and repair, it is important to enable localized, controlled delivery of active agents, whose concentrations and bioavailability can be closely regulated to achieve significant and predictable cellular responses. Delivery of active agents from polymeric carriers, such as microparticle and nanoparticle (NP) carriers is being widely investigated for various *in vivo* drug delivery applications (Lee et al., 2000; Soppimath et al., 2001; Allen and Cullis 2004). Compared to other delivery modes such as those involving the use of microparticles, NPs offer several advantages, including higher drug release rates due to their higher surface area/unit volume, improved tissue infiltration and interaction at the cellular level due to their nano-range sizes

(Shive and Anderson 1997; Flemming et al., 1999; Wu 2004), and generation of small amounts of byproducts of polymer degradation that can potentially have adverse effects on cell viability or health (Panyam et al., 2003).

In this study, we evaluated the effects of localized delivery of active agents from PLGA) NPs, on the *in vitro* elastogenic induction of human aortic smooth muscle cells (HASMCs) seeded within a tubular collagen gel 3-D tissue microenvironment, a system wherein we have previously investigated auto-generation of elastic matrix by seeded cells (Venkataraman and Ramamurthi 2011). The biodegradability of PLGA and its biocompatibility, as well as its ease of formulation and characterization have led the FDA to approve its use as a vehicle for drug delivery (Astete and Sabliov 2006; Lu et al., 2009). PLGA undergoes hydrolytic degradation into lactic and glycolic acid, which have been demonstrated to be non-cytotoxic, both *in vitro* and *in vivo* (Astete and Sabliov 2006). PLGA composed of a 50:50 lactide:glycolide ratio is the primary type of PLGA used in biomedical applications, including drug delivery systems, as it degrades faster (50-60 days) than either polylactic acid (PLA) or polyglycolic acid (PGA) (Lu et al., 2009). It has been used to deliver both DOX (Patel et al., 2012; Wang et al., 2012; Sivaraman and Ramamurthi 2013) and TGF-β1 (Lu et al., 2000; Jaklenec et al., 2008). For our studies, we thus formulated NPs using high molecular weight (MW = 117.7 kDa) PLGA containing a 50:50 lactide:glycolide ratio. Since PLGA of this higher MW PLGA exhibits a slower degradation rate compared to lower MW PLGA (Song et al., 1997), we expected that with its use, we could achieve sustained delivery of therapeutic agents over longer periods of time.

The method of formulation of NPs critically controls their size and surface charge, with single- or double emulsion solvent evaporation methods being the most common methods used (Astete and Sabliov 2006; Lu et al., 2009). The double emulsion method, which involves the formation of a water-in-oil-in-water emulsion, is ideal to encapsulate water-soluble drugs. This method was thus utilized for the encapsulation of both TGF-β1 and DOX. As stated earlier in the methods, the aqueous stabilizer used during NP formulation imparts the surface of PLGA NPs with a distinct charge, and concurrently stabilizes the polymer-drug emulsion to form NPs (rather than microparticles) of uniform sizes. PVA, which is a non-ionic surfactant (Peetla and Labhasetwar 2009) widely used in the formulation of biodegradable PLGA NPs, imparts the NPs with a negative surface charge (ζ-potential = -28 mV), as we have shown in recent studies (Sivaraman and Ramamurthi 2013; Sylvester et al.,). We sought to generate negatively-charged NPs which would remain in the extracellular space due to electrostatic repulsion by the cell surface which carries a net negative charge. This would be beneficial to influencing cellular elastin synthesis via release of active agents from the NPs, without them actually infiltrating the cells, which could have potential negative implications (Panyam and Labhasetwar 2003). Both the agent-loaded and agent-free NPs we formulated exhibited a negative surface charge between -26 and -31 mV, with a mean hydrodynamic diameter in the range of 300-350 nm. This NP size was particularly suited for our application, as NPs < 100 nm and > 500 nm have been shown to trigger an immune (Busch et al., 2011) or phagocytic response *in vivo* (Nguyen et al., 2009).

The encapsulation efficiency of TGF-β1 was relatively high (84.0 ± 9.0 %) for the different TGF-β1 loadings; Table 1), which was higher than that of the 25-40% entrapment

efficiencies obtained in other studies using PLGA as the carrier (Lu et al., 2001; Jhunjhunwala et al., 2012), but comparable to the 83% entrapment efficiency (Lu et al., 2000) for TGF-β1 encapsulation within PLGA microparticles. However, the encapsulation efficiency of DOX was lower (~58%; Table 2), which could be attributed to its highly water-soluble nature, as hydrophilic drugs demonstrate a lower affinity for PLGA (Tewes et al., 2007) due to its hydrophobic nature. On account of this, such drugs tend to partition into the aqueous phase instead of the organic (polymer) phase (Govender et al., 1999; Cohen-Sela et al., 2009), resulting in their lower encapsulation within the polymer carrier matrix.

Previous studies by our group and others have shown TGF-β1 to stimulate elastic matrix synthesis (Losy et al., 2003; Kothapalli et al., 2009; Kothapalli et al., 2009) in a dose-dependent manner, though it is also known that its excess bioavailability can adversely impact cells by inducing apoptosis and augmenting cellular processes leading to matrix mineralization (Brown et al., 2002; Simionescu et al., 2005). In this context, localized, controlled, and steady-state delivery of TGF-β1 from PLGA NPs would be beneficial to limit its bioavailability in the cellular microenvironment. Similarly, there is need to deliver DOX in a controlled and localized manner, since it has been shown to generate side effects when delivered systemically (Baxter et al., 2002), while also inhibiting MMPs, which play a role in normal matrix turnover in healthy tissues, which is undesirable (Galis and Khatri 2002). This is further emphasized by recent peripheral evidence that systemic DOX delivery leads to inhibited elastic matrix deposition by vascular SMCs (Bendeck et al., 2002; Franco et al., 2006), and evidence from our own studies (Sivaraman and Ramamurthi 2013) that DOX delivery from NPs at steady state concentrations in the low μg/mL range provides functional benefits *in vitro* in terms of MMP inhibition parallel with augmentation of elastic matrix deposition.

TGF-β1 and DOX (Figures 2A and B) exhibited a characteristic release profile, which has also been observed for the release of other drugs from PLGA NPs (Labhasetwar et al., 1998; Panyam et al., 2003). The release profile was characterized by an initial burst phase ending within the first 24 h, followed by a slower exponential release phase that extended over several more days before plateauing (Figure 2A) at ~7 days. Since in the TGF-β1 release study, the concentration of TGF-β1-loaded PLGA NPs (10 mg/mL at 2000 ng of TGF-β1 loading) was far higher than that delivered in our subsequent cell culture studies (0.3 mg/mL), the TGF-β1 release in the latter was likely ~33-fold lower (i.e., 0.2 ng/mL) than the 6.5 ng/mL steady-state concentration generated for this formulation in the release-studies (see Figure 2A).

In the case of DOX, its release during the initial burst phase was higher (ranging between 5.7 μg/mL for 2% DOX loaded NPs at 0.2 mg/mL to 10.6 μg/mL for 5% DOX-loaded NPs at 0.5 mg/mL) than the dose of ~ 5.0 μg/mL that we had observed in unpublished pilot studies to inhibit SMC proliferation and elastic matrix synthesis in aneurysmal rat aortic SMC cultures. However, when cultured with DOX-releasing NPs, neither the DOX, nor the NPs themselves impacted HASMC viability (Supplementary Figure 3), and proliferation and elastic matrix synthesis adversely, as shown in Figures 3 and 5B, respectively. The lack of any such adverse effects may likely have been due to only short, temporal exposure of cells to DOX doses > 5 μg/mL during the initial burst phase and their exposure to DOX at doses

(2.5-4.8 μg/mL) significantly below this threshold value, over the remaining culture period of 20 days. Regardless, these results suggest that transient burst release of DOX from these NPs is not a concern from the standpoint of cellular health. Extrapolating from our release curves in Figure 2A, we anticipate the release of TGF-β1 from NPs (2000 ng loading, 0.3 ng/mL NP concentration) during the initial 24 h burst phase to be ~0.15 ng/mL. This dose was determined to be non-cytotoxic when provided alone, or together with DOX to HASMCs, which might be expected in light of our published data which shows no cytotoxicity of TGF-β1 even at a 10 ng/mL dose (Gacchina et al., 2011).

The absence of any differences in expression of genes for contractile SMC markers and for osteopontin (a marker typically only expressed by activated SMCs) between BNP and ANP-supplemented HASMC cultures, suggests the lack of SMC activation or phenotypic alteration by our delivered active agents. On the other hand, the lack of differences between cultures treated with exogenous agents (EDC) and the ANP, suggest that the nanoparticle carriers do not have any adverse effects on cellular phenotype or health. Consistent with gene expression data, western blots (Supplementary Figure 4A) also showed no apparent differences in β-actin band intensities corresponding to the SMC marker proteins by HASMCs cultured with both exogenous agents and NPs.

We observed expression of genes for elastin and other proteins important to elastic fiber assembly (fibrillin-1, fibulin-5) to be upregulated in ANP and EDC cultures relative to that in BNP cultures that did not receive TGF-β1 and DOX. Based on our recent published study (Sivaraman et al., 2013) wherein we showed DOX released from NPs to have no significant effect on tropoelastin or matrix elastin synthesis on a per cell basis, we attribute the upregulated elastin gene expression in agent-delivered cultures to effects of TGF-β1 (Figure 5A). The stimulatory effect of TGF-β1 on elastin synthesis, both at the mRNA and protein levels, has been demonstrated in various in vitro models, including in our own studies (Liu and Davidson 1988; Kothapalli et al., 2009) and appears to primarily involve stabilization of elastin mRNA (Kahari et al., 1992; Davidson et al., 2007), although a TGFβ1–responsive element has been identified in the human elastin promoter (Marigo et al., 1993; Marigo et al., 1994).

Gene expression of LOX, an enzyme involved in crosslinking elastin precursors in matrix structures was enhanced in cultures that received NPs (both BNPs and ANPs) over that in EDC cultures (Figure 5A). Also, LOX gene expression was almost identical in BNP and ANP cultures. These outcomes suggest that the NPs, independent of the active agents, augment the elastin crosslinking aspect. In support of this, our western blot data for LOX protein (where detectable; see Supplementary Figure 4B) showed higher levels of LOX synthesis (normalized to β-actin) in BNP and ANP-supplemented cultures relative to the EDC cultures. Despite this supporting evidence, the mechanism(s) underlying NP-induced upregulation of LOX gene expression and protein synthesis are highly unclear and warrant future study. At this point, it may however be hypothesized that (a) the limited infiltration of the NPs into cells, and/or (b) cellular uptake of or cellular microenvironmental changes due to PLGA degradation byproducts (i.e., lactic and glycolic acids) or PVA could trigger intracellular cascades leading to downstream effects of augmented LOX gene expression/ mRNA stability, and LOX protein synthesis. Taken together, our gene expression data

suggests that active agent exposure is beneficial to elastin protein synthesis itself, while NP delivery serves to enhance the matrix crosslinking aspect. The former effect however likely dominates and determines elastic matrix deposition since our data for matrix elastin content, as measured by the Fastin assay (Figure 5B) shows a ~2-fold increase in total matrix elastin in ANP- and EDC-treated cultures relative to that in BNP-treated cultures.

Matrix elastin content was significantly higher in ANP-supplemented constructs than in BNP-supplemented constructs clearly emphasizing the pro-elastogenic benefits of released DOX and TGF-β1. On the other hand, matrix elastin production in EDC and ANP constructs were very similar. This outcome is highly significant because despite the equivalence between exogenous delivery doses of TGF-β1 and DOX and their doses delivered from the NPs (see section 2.8), the total amounts of TGF-β1 (10 ng) and DOX (570 μg) delivered in the exogenous mode over 21 days of culture was in fact, 20-fold greater than that released from the NPs (0.5 ng and 28.5 μg respectively, assuming 100% NP retention within the collagen constructs as a highly conservative estimate). The amounts of the active agents delivered in the exogenous case were higher due to replenishment of new medium with agents every two days (10 medium changes over 21 days of culture). More specifically, the total amounts of exogenous agents delivered were calculated based on 5 mL of medium per medium change per construct, and a total of 10 medium changes over the culture period for added doses of 0.2 ng/mL of TGF-β1 and 11.4 μg/mL of DOX. A more realistic assumption of less than 100% NP retention within the constructs would suggest that NP-released amounts of the active agents within are even lower than the amounts estimated above from the release curves, assuming 100% NP retention. These results thus clearly emphasize that active agent amounts necessary to evoke the same elastogenic effects are far lower when they are delivered using NPs than when they are exogenously dosed. It must be noted that the process of ECM assembly is complex, and the duration required for deposition of a mature elastic matrix by SMCs is on the order of ~21 days, as shown in a recent study by our group (Gacchina and Ramamurthi, 2011). The NPs serve as a reservoir of the active agents, releasing them in a controlled manner over 21 days (Figure 2), indicating that agents released from NPs remain bioavailable (and also bioactive), thereby enabling the generation of functional elastic matrix within the collagenous constructs. As seen in Figure 5A, the total amount of elastic matrix generated within the ANP-treated cultures over this duration, was approximately 2-fold higher than that obtained in cultures treated with BNPs, illustrating the elastogenic benefits of the controlled release of these agents from NPs at 20-fold lower concentrations compared to EDC. This benefit is expected to be accentuated for longer culture durations, as evidenced by the fact that their steady-state release may be extended up to 60 days, as shown in the case of DOX in Supplementary Figure S1.

Additionally, visual analysis of elastin and elastic matrix within the constructs (Elastic stain in Figure 7 and Immunofluorescence imaging in Figure 8) did not reveal obvious differences between the three treatment conditions. The ultrastructure of all constructs showed a higher degree of longitudinal orientation than circumferential alignment, likely due the application of low strains. Circumferential alignment of cells and elastic matrix were however found in regions closer to the lumen of the tubular constructs.

Both the anionic BNP- and ANP-treated constructs demonstrated a marked increase in MMP2 mRNA expression, protein synthesis, and enzyme activity, compared to EDC-treated constructs (Figures 6A-E). However, it must be noted that the delivery of active agents from the NPs resulted in a decrease in overall MMP2 mRNA expression in the ANP-treated constructs relative to BNP-treated constructs (Figure 6A), illustrating the positive influence of the active agents in attenuating MMP2 gene expression. The overall increase in MMP2 gene expression in NP-treated constructs vs. EDC-constructs is consistent with observations made upon exposure of other cell types such as gingival fibroblasts to anionic NPs (Naveau et al., 2006). As noted in that prior study, here too, it is certainly possible that a transient inflammatory response is incited by our NPs, characterized by increased production of cytokines, which in turn may have served to induce MMP-2 transcription. On the other hand, increased synthesis and activity of active MMP-2 in NP-treated constructs (Figure 6B) may be attributed to electrostatic attraction-based interactions of anionic NPs with MMPs that carry a net positive charge (primarily due to the presence of a cationic Zn^{2+} ion at its active site) (Gertler 1971; Takahashi et al., 2005). Although MMP-2 enzyme activity was lower in ANP-treated constructs compared to BNP-treated constructs (Figure 6E), it remained higher than the constructs treated with exogenous DOX and TGF-β1. These outcomes are not unexpected, and may be attributable to the inability of the DOX released from the NPs (11.4 μg/mL over 21 days) to overcome the enhanced upregulation of MMP-2 at the gene and protein levels due to the electrostatic interactions of the anionic NPs with the net positively-charged MMP-2. Additionally, the exogenous amount of DOX dosed over the 21-day duration of the culture (570 μg; 20-fold higher than the total amount of DOX released from NPs within the construct) would be expected to be highly effective in inhibiting MMP-2 production and activity in the EDC-treated constructs.

Studies by other groups have shown decreased MMP-2 activity due to electrostatic repulsion of the negative-charged glutamic acid residues within its active site, and essential to its activity, by anionic drug-conjugates (Visse and Nagase 2003; Chau et al., 2004). However, it must also be noted that the effects of cationic compounds in inhibiting MMP-2 production and activity studies has been shown contradictorily in numerous other studies (Gendron et al., 1999; Ganguly et al., 2007; Mendis et al., 2009; Tezvergil-Mutluay et al., 2011). In fact, a recent study by our own group (Sivaraman and Ramamurthi 2013), showed that cationic functionalization of NPs is conducive to attenuated MMP-2 synthesis and activity. However, in these latter studies, consideration must be given to the fact that the cationic compounds all contained long-alkyl chains which could have contributed strongly to MMP inhibition via steric blockade of its active site, as hypothesized in our earlier work (Sivaraman and Ramamurthi 2013). Nevertheless, collectively our results suggest that a fine line exists in terms of interactions and consequent effects of charge of NP surface moieties with the regulation of MMP2 synthesis and activity, which mandates a further dedicated investigation.

In contrast to MMP-2, the mRNA expression, total protein content and enzymatic activity of MMP-9 was found to be significantly lower in constructs cultured with BNPs and ANPs relative to EDC-treated constructs (Figures 6A-E). The lack of difference in the MMP-9 protein levels (as seen in western blots; Figures 6C and D) between BNP- and ANP-treated cultures suggests that active agent delivery from the NPs did not have any significant effect

on MMP-9 synthesis. In addition to this, zymogen bands for MMP-9 enzyme were completely undetected in both sets of the NP-treated constructs, unlike the EDC-treated constructs which showed a distinct band corresponding to active MMP-9 (Figures 6D and E). We hypothesize that this may be attributed to either (a) the ability of these anionic NPs to attenuate MMP-9 synthesis and activity in ANP- and BNP-treated cultures, or alternatively, (b) the ability of the exogenously dosed DOX and TGF-β1 to activate MMP-9, although the exact mechanisms underlying these distinct phenomena remain unclear. Since DOX would be expected to inhibit MMP-9 on account of its MMP-inhibitory properties (Uitto et al., 1994; Boyle et al., 1998; Hanemaaijer et al., 1998; Thompson and Baxter 1999; Kim et al., 2005; Bedi et al., 2010; Stechmiller et al., 2010), we hypothesize that the exogenous dosage of TGF-β1 potentially mediates intracellular signaling events/cascades which culminate in increased activation of MMP-9, but not MMP-2. This would then be consistent with results obtained by other groups, which have demonstrated the ability of TGF-β1 to activate MMP-9 but not MMP-2, albeit in cancer cell lines (Welch et al., 1990; Samuel et al., 1992; Sehgal et al., 1996). However, studies have demonstrated the ability of DOX to inhibit TGF-β1 induced activation of MMP-9 in human corneal epithelial cells (Kim et al., 2005). Hence, this suggests that the attenuation of MMP-9 synthesis and activity is likely to be mediated by the anionic NPs present within the constructs, again providing evidence as to a role for NP surface charge in regulating MMP synthesis and activity. Future studies will need to focus on the mechanistic basis for these effects.

5. Conclusions

Our results show that DOX- and TGF-β1 released from PLGA NPs positively influences elastogenic outcomes for HASMCs within tubular collagen constructs, and generates outcomes comparable to that induced by exogenous medium supplements of DOX and TGF-β1. The overarching significance of this study however lies in the fact that for equivalent release concentrations of these agents, the total amount of active agents released from the NPs over a 21 day period of culture was ~20-fold lower than the amount of active agents dosed exogenously. This clearly illustrates that controlled, sustained delivery of pro-elastogenic factors from scaffold-embedded polymeric NPs is a more efficient strategy for directed elastogenesis, particularly in longer-term cultures demanded of for generation of mature tissue constructs. Although the anionic NPs used in this study caused a moderate upregulation of MMP-2 synthesis and activity, they exerted a significant inhibitory effect on MMP-9 synthesis and activity by the HASMCs. Based on this study, as well as other recent studies in our laboratory, future work will evaluate the functional benefits of delivery of these active agents from cationically- and anionically-functionalized PLGA NPs, towards enhancing elastogenic induction and attenuating MMP production and activity *in vitro,* as well as *in vivo* within rat AAAs.

Supplementary Material

Refer to Web version on PubMed Central for supplementary material.

Acknowledgments

This study was supported by NIH Grants: National Heart, Lung, and Blood Institute (5R01HL 092051-02)

References

Allen TM, Cullis PR. Drug delivery systems: Entering the mainstream. Science. 2004; 303:1818–1822. [PubMed: 15031496]

Annambhotla S, Bourgeois S, Wang X, Lin PH, Yao Q, Chen C. Recent advances in molecular mechanisms of abdominal aortic aneurysm formation. World J Surg. 2008; 32:976–986. [PubMed: 18259804]

Astete CE, Sabliov CM. Synthesis and characterization of PLGA nanoparticles. J Biomater Sci Polym Ed. 2006; 17:247–289. [PubMed: 16689015]

Bartoli MA, Parodi FE, Chu J, Pagano MB, Mao D, Baxter BT, Buckley C, Ennis TL, Thompson RW. Localized administration of doxycycline suppresses aortic dilatation in an experimental mouse model of abdominal aortic aneurysm. Ann Vasc Surg. 2006; 20:228–236. [PubMed: 16572291]

Bartoli MA, Parodi FE, Chu J, Pagano MB, Mao DL, Baxter BT, Buckley C, Ennis TL, Thompson RW. Localized administration of doxycycline suppresses aortic dilatation in an experimental mouse model of abdominal aortic aneurysm. Ann Vasc Surg. 2006; 20:228–236. [PubMed: 16572291]

Battegay EJ, Raines EW, Seifert RA, Bowen-Pope DF, Ross R. TGF-beta induces bimodal proliferation of connective tissue cells via complex control of an autocrine PDGF loop. Cell. 1990; 63:515–524. [PubMed: 2171777]

Baxter BT, Pearce WH, Waltke EA, Littooy FN, Hallett JW Jr, Kent KC, Upchurch GR Jr, Chaikof EL, Mills JL, Fleckten B, Longo GM, Lee JK, Thompson RW. Prolonged administration of doxycycline in patients with small asymptomatic abdominal aortic aneurysms: report of a prospective (Phase II) multicenter study. J Vasc Surg. 2002; 36:1–12. [PubMed: 12096249]

Baxter BT, Pearce WH, Waltke EA, Littooy FN, Hallett JW, Kent KC, Upchurch GR, Chaikof EL, Mills JL, Fleckten B, Longo GM, Lee JK, Thompson RW. Prolonged administration of doxycycline in patients with small asymptomatic abdominal aortic aneurysms: Report of a prospective (Phase II) multicenter study. J Vasc Surg. 2002; 36:1–12. [PubMed: 12096249]

Bedi A, Fox AJS, Kovacevic D, Deng Xh, Warren RF, Rodeo SA. Doxycycline-Mediated Inhibition of Matrix Metalloproteinases Improves Healing After Rotator Cuff Repair. Am J Sports Med. 2010; 38:308–317. [PubMed: 19826139]

Bendeck MP, Conte M, Zhang M, Nili N, Strauss BH, Farwell SM. Doxycycline modulates smooth muscle cell growth, migration, and matrix remodeling after arterial injury. Am J Pathol. 2002; 160:1089–1095. [PubMed: 11891205]

Bendeck MP, Conte M, Zhang MY, Nili N, Strauss BH, Farwell SM. Doxycycline modulates smooth muscle cell growth, migration, and matrix remodeling after arterial injury. Am J Pathol. 2002; 160:1089–1095. [PubMed: 11891205]

Blanchard JF. Epidemiology of abdominal aortic aneurysms. Epidemiol Rev. 1999; 21:207–221. [PubMed: 10682258]

Boyle JR, McDermott E, Crowther M, Wills AD, Bell PRF, Thompson MM. Doxycycline inhibits elastin degradation and reduces metalloproteinase activity in a model of aneurysmal disease. Journal of Vascular Surgery. 1998; 27:354–361. [PubMed: 9510291]

Brown RA, Sethi KK, Gwanmesia I, Raemdonck D, Eastwood M, Mudera V. Enhanced fibroblast contraction of 3D collagen lattices and integrin expression by TGF-beta 1 and -beta 3: Mechanoregulatory growth factors? Exp Cell Res. 2002; 274:310–322. [PubMed: 11900491]

Busch W, Bastian S, Trahorsch U, Iwe M, Kühnel D, Meiβner T, Springer A, Gelinsky M, Richter V, Ikonomidou C, Potthoff A, Lehmann I, Schirmer K. Internalisation of engineered nanoparticles into mammalian cells in vitro: influence of cell type and particle properties. J Nanopart Res. 2011; 13:293–310.

Chadwick, D.; Goode, J. Ciba Foundation. The molecular biology and pathology of elastic tissues. Chichester; New York: J. Wiley; 1995.

Chau Y, Tan FE, Langer R. Synthesis and characterization of dextran-peptide-methotrexate conjugates for tumor targeting via mediation by matrix metalloproteinase II and matrix metalloproteinase IX. Bioconjug Chem. 2004; 15:931–941. [PubMed: 15264885]

Cohen-Sela E, Chorny M, Koroukhov N, Danenberg HD, Golomb G. A new double emulsion solvent diffusion technique for encapsulating hydrophilic molecules in PLGA nanoparticles. J Control Release. 2009; 133:90–95. [PubMed: 18848962]

Curci JA, Mao DL, Bohner DG, Allen BT, Rubin BG, Reilly JM, Sicard GA, Thompson RW. Preoperative treatment with doxycycline reduces aortic wall expression and activation of matrix metalloproteinases in patients with abdominal aortic aneurysms. J Vasc Surg. 2000; 31:325–341. [PubMed: 10664501]

Curci JA, Petrinec D, Liao SX, Golub LM, Thompson RW. Pharmacologic suppression of experimental abdominal aortic aneurysms: A comparison of doxycycline and four chemically modified tetracyclines. J Vasc Surg. 1998; 28:1082–1093. [PubMed: 9845660]

Daugherty A, Cassis LA. Mechanisms of abdominal aortic aneurysm formation. Curr Atheroscler Rep. 2002; 4:222–227. [PubMed: 11931720]

Davda J, Labhasetwar V. Sustained Proangiogenic Activity of Vascular Endothelial Growth Factor Following Encapsulation in Nanoparticles. J Biomed Nanotechnol. 2005; 1:74–82.

Davidson, JM.; Zang, MC.; Zoia, O.; Giro, MG. Ciba Foundation Symposium 192 - The Molecular Biology and Pathology of Elastic Tissues. John Wiley & Sons, Ltd.; 2007. Regulation of Elastin Synthesis in Pathological States; p. 81-99.

Davies AK, Cundall RB, Dandiker Y, Slifkin MA. Photo-oxidation of tetracycline adsorbed on hydroxyapatite in relation to the light-induced staining of teeth. J Dent Res. 1985; 64:936–939. [PubMed: 2987327]

Flemming RG, Murphy CJ, Abrams GA, Goodman SL, Nealey PF. Effects of synthetic micro- and nano-structured surfaces on cell behavior. Biomaterials. 1999; 20:573–588. [PubMed: 10213360]

Franco C, Ho B, Mulholland D, Hou GP, Islam M, Donaldson K, Bendeck MP. Doxycycline alters vascular smooth muscle cell adhesion, migration, and reorganization of fibrillar collagen matrices. Am J Pathol. 2006; 168:1697–1709. [PubMed: 16651635]

Gacchina CE, Brothers TE, Ramamurthi A. Evaluating Smooth Muscle Cells from CaCl2-Induced Rat Aortal Expansions as a Surrogate Culture Model for Study of Elastogenic Induction of Human Aneurysmal Cells. Tissue Eng. 2011; 17:1945–1948.

Gacchina CE, Deb PP, Barth JL, Ramamurthi A. Elastogenic Inductability of Smooth Muscle Cells from a Rat Model of Late Stage Abdominal Aortic Aneurysms. Tissue Eng. 2011; 17:1699–1711.

Gacchina CE, Ramamurthi A. Impact of pre-existing elastic matrix on TGFβ1 and HA oligomer-induced regenerative elastin repair by rat aortic smooth muscle cells. J Tissue Eng Regen Med. 2011; 5:85–96. [PubMed: 20653044]

Galis ZS, Khatri JJ. Matrix metalloproteinases in vascular remodeling and atherogenesis - The good, the bad, and the ugly. Circ Res. 2002; 90:251–262. [PubMed: 11861412]

Galis ZS, Khatri JJ. Matrix metalloproteinases in vascular remodeling and atherogenesis: the good, the bad, and the ugly. Circ Res. 2002; 90:251–262. [PubMed: 11861412]

Ganguly B, Banerjee J, Elegbede AI, Klocke DJ, Mallik S, Srivastava DK. Intrinsic selectivity in binding of matrix metalloproteinase-7 to differently charged lipid membranes. FEBS Lett. 2007; 581:5723–5726. [PubMed: 18036564]

Gendron R, Grenier D, Sorsa T, Mayrand D. Inhibition of the activities of matrix metalloproteinases 2, 8, and 9 by chlorhexidine. Clin Diagn Lab Immunol. 1999; 6:437–439. [PubMed: 10225852]

Gertler A. The non-specific electrostatic nature of the adsorption of elastase and other basic proteins on elastin. Eur J Biochem. 1971; 20:541–546. [PubMed: 5104188]

Govender T, Stolnik S, Garnett MC, Illum L, Davis SS. PLGA nanoparticles prepared by nanoprecipitation: drug loading and release studies of a water soluble drug. J Control Release. 1999; 57:171–185. [PubMed: 9971898]

Guzman LA, Labhasetwar V, Song CX, Jang YS, Lincoff AM, Levy R, Topol EJ. Local intraluminal infusion of biodegradable polymeric nanoparticles - A novel approach for prolonged drug delivery after balloon angioplasty. Circulation. 1996; 94:1441–1448. [PubMed: 8823004]

Haerdi-Landerer MC, Suter MM, Steiner A, Wittenbrink MM, Pickl A, Gander BA. In vitro cell compatibility and antibacterial activity of microencapsulated doxycycline designed for improved localized therapy of septic arthritis. J Antimicrob Chemother. 2008; 61:332–340. [PubMed: 18174200]

Hanemaaijer R, Visser H, Koolwijk P, Sorsa T, Salo T, Golub LM, van Hinsbergh VW. Inhibition of MMP synthesis by doxycycline and chemically modified tetracyclines (CMTs) in human endothelial cells. Adv Dent Res. 1998; 12:114–118. [PubMed: 9972133]

Honnorat-Benabbou VC, Lebugle AA, Sallek B, Duffaut-Lagarrigue D. Stability study of tetracyclines with respect to their use in slow release systems. J Mater Sci Mater Med. 2001; 12:107–110. [PubMed: 15348315]

Injac R, Kac J, Kreft S, Strukelj B. Determination of doxycycline in pharmaceuticals and human urine by micellar electrokinetic capillary chromatography. Anal Bioanal Chem. 2007; 387:695–701. [PubMed: 17102968]

Jaklenec A, Hinckfuss A, Bilgen B, Ciombor DM, Aaron R, Mathiowitz E. Sequential release of bioactive IGF-I and TGF-beta 1 from PLGA microsphere-based scaffolds. Biomaterials. 2008; 29:1518–1525. [PubMed: 18166223]

Jhunjhunwala S, Balmert SC, Raimondi G, Dons E, Nichols EE, Thomson AW, Little SR. Controlled release formulations of IL-2, TGF-beta 1 and rapamycin for the induction of regulatory T cells. J Control Release. 2012; 159:78–84. [PubMed: 22285546]

Kahari VM, Olsen DR, Rhudy RW, Carrillo P, Chen YQ, Uitto J. Transforming growth factor-beta up-regulates elastin gene expression in human skin fibroblasts. Evidence for post-transcriptional modulation. Lab Invest. 1992; 66:580–588. [PubMed: 1573852]

Kim BS, Nikolovski J, Bonadio J, Smiley E, Mooney DJ. Engineered smooth muscle tissues: Regulating cell phenotype with the scaffold. Exp Cel Res. 1999; 251:318–328.

Kim HS, Luo LH, Pflugfelder SC, Li DQ. Doxycycline inhibits TGF-beta 1-induced MMP-9 via Smad and MAPK pathways in human corneal epithelial cells. Invest Ophthalmol Vis Sci. 2005; 46:840–848. [PubMed: 15728539]

Kothapalli CR, Gacchina CE, Ramamurthi A. Utility of hyaluronan oligomers and transforming growth factor-beta1 factors for elastic matrix regeneration by aneurysmal rat aortic smooth muscle cells. Tissue Eng Part A. 2009; 15:3247–3260. [PubMed: 19374489]

Kothapalli CR, Gacchina CE, Ramamurthi A. Utility of Hyaluronan Oligomers and Transforming Growth Factor-Beta1 Factors for Elastic Matrix Regeneration by Aneurysmal Rat Aortic Smooth Muscle Cells. Tissue Eng. 2009; 15:3247–3260.

Kothapalli CR, Taylor PM, Smolenski RT, Yacoub MH, Ramamurthi A. Transforming growth factor beta 1 and hyaluronan oligomers synergistically enhance elastin matrix regeneration by vascular smooth muscle cells. Tissue Eng Part A. 2009; 15:501–511. [PubMed: 18847364]

Kothapalli CR, Taylor PM, Smolenski RT, Yacoub MH, Ramamurthi A. Transforming Growth Factor Beta 1 and Hyaluronan Oligomers Synergistically Enhance Elastin Matrix Regeneration by Vascular Smooth Muscle Cells. Tissue Eng. 2009; 15:501–511.

L'Heureux N, Germain L, Labbe R, Auger FA. In vitro construction of a human blood vessel from cultured vascular cells. J Vasc Surg. 1993; 17:499–509. [PubMed: 8445745]

Labarca C, Paigen K. A simple, rapid, and sensitive DNA assay procedure. Anal Biochem. 1980; 102:344–352. [PubMed: 6158890]

Labhasetwar V, Song CX, Humphrey W, Shebuski R, Levy RJ. Arterial uptake of biodegradable nanoparticles: Effect of surface modifications. J Pharm Sci. 1998; 87:1229–1234. [PubMed: 9758682]

Lee KY, Peters MC, Anderson KW, Mooney DJ. Controlled growth factor release from synthetic extracellular matrices. Nature. 2000; 408:998–1000. [PubMed: 11140690]

Li DY, Brooke B, Davis EC, Mecham RP, Sorensen LK, Boak BB, Eichwald E, Keating MT. Elastin is an essential determinant of arterial morphogenesis. Nature. 1998; 393:276–280. [PubMed: 9607766]

Liu JM, Davidson JM. The elastogenic effect of recombinant transforming growth factor-beta on porcine aortic smooth muscle cells. Biochem Biophys Res Commun. 1988; 154:895–901. [PubMed: 3165637]

Livak KJ, Schmittgen TD. Analysis of relative gene expression data using real-time quantitative PCR and the 2(T)(-Delta Delta C) method. Methods. 2001; 25:402–408. [PubMed: 11846609]

Losy F, Dai JP, Pages C, Ginat M, Muscatelli-Groux B, Guinault AM, Rousselle E, Smedile G, Loisance D, Becquemin JP, Allaire E. Paracrine secretion of transforming growth factor-beta(1) in aneurysm healing and stabilization with endovascular smooth muscle cell therapy. J Vasc Surg. 2003; 37:1301–1309. [PubMed: 12764279]

Lu JM, Wang X, Marin-Muller C, Wang H, Lin PH, Yao Q, Chen C. Current advances in research and clinical applications of PLGA-based nanotechnology. Expert Rev Mol Diagn. 2009; 9:325–341. [PubMed: 19435455]

Lu L, Stamatas GN, Mikos AG. Controlled release of transforming growth factor beta1 from biodegradable polymer microparticles. J Biomed Mater Res. 2000; 50:440–451. [PubMed: 10737887]

Lu L, Stamatas GN, Mikos AG. Controlled release of transforming growth factor beta 1 from biodegradable polymer microparticles. J Biomed Mater Res. 2000; 50:440–451. [PubMed: 10737887]

Lu LC, Yaszemski MJ, Mikos AG. TGF-beta 1 release from biodegradable polymer microparticles: Its effects on marrow stromal osteoblast function. J Bone Joint Surg Am. 2001; 83A:S82–S91.

Manning MW, Cassis LA, Daugherty A. Differential effects of doxycycline, a broad-spectrum matrix metalloproteinase inhibitor, on angiotensin II-induced atherosclerosis and abdominal aortic aneurysms. Arterioscler Thromb Vasc Biol. 2003; 23:483–488. [PubMed: 12615694]

Marigo V, Volpin D, Bressan GM. Regulation of the human elastin promoter in chick embryo cells. Tissue-specific effect of TGF-beta. Biochim Biophys Acta. 1993; 20:1–2.

Marigo V, Volpin D, Vitale G, Bressan GM. Identification of a TGF-beta responsive element in the human elastin promoter. Biochem Biophys Res Commun. 1994; 199:1049–1056. [PubMed: 8135778]

Marshall OJ. PerlPrimer: cross-platform, graphical primer design for standard, bisulphite and real-time PCR. Bioinformatics. 2004; 20:2471–2472. [PubMed: 15073005]

Mendis E, Kim MM, Rajapakse N, Kim SK. The inhibitory mechanism of a novel cationic glucosamine derivative against MMP-2 and MMP-9 expressions. Bioorg Med Chem Lett. 2009; 19:2755–2759. [PubMed: 19375915]

Mitic SS, Miletic GZ, Kostic DA, Naskovic-Dokic DC, Arsic BB, Rasic ID. A rapid and reliable determination of doxycycline hyclate by HPLC with UV detection in pharmaceutical samples. J Serb Chem Soc. 2008; 73:665–671.

Naveau A, Smirnov P, Menager C, Gazeau F, Clement O, Lafont A, Gogly B. Phenotypic study of human gingival fibroblasts labeled with superparamagnetic anionic nanoparticles. J Periodontol. 2006; 77:238–247. [PubMed: 16460250]

Nguyen KT, Shukla KP, Moctezuma M, Braden ARC, Zhou J, Hu ZB, Tang LP. Studies of the cellular uptake of hydrogel nanospheres and microspheres by phagocytes, vascular endothelial cells, and smooth muscle cells. J Biomed Mater Res. 2009; 88A:1022–1030.

Panyam J, Dali MA, Sahoo SK, Ma WX, Chakravarthi SS, Amidon GL, Levy RJ, Labhasetwar V. Polymer degradation and in vitro release of a model protein from poly(D,L-lactide-co-glycolide) nano- and microparticles. J Control Release. 2003; 92:173–187. [PubMed: 14499195]

Panyam J, Labhasetwar V. Biodegradable nanoparticles for drug and gene delivery to cells and tissue. Adv Dru Deliv Rev. 2003; 55:329–347.

Patel A, Fine B, Sandig M, Mequanint K. Elastin biosynthesis: The missing link in tissue-engineered blood vessels. Cardiovasc Res. 2006; 71:40–49. [PubMed: 16566911]

Patel RS, Cho DY, Tian C, Chang A, Estrellas KM, Lavin D, Furtado S, Mathiowitz E. Doxycycline delivery from PLGA microspheres prepared by a modified solvent removal method. J Microencapsul. 2012; doi: 10.3109/02652048.2011.651499

Peetla C, Labhasetwar V. Effect of Molecular Structure of Cationic Surfactants on Biophysical Interactions of Surfactant-Modified Nanoparticles with a Model Membrane and Cellular Uptake. Langmuir. 2009; 25:2369–2377. [PubMed: 19161268]

Prall AK, Longo GM, Mayhan WG, Waltke EA, Fleckten B, Thompson RW, Baxter BT. Doxycycline in patients with abdominal aortic aneurysms and in mice: Comparison of serum levels and effect on aneurysm growth in mice. J Vasc Surg. 2002; 35:923–928. [PubMed: 12021708]

Samuel SK, Hurta RA, Kondaiah P, Khalil N, Turley EA, Wright JA, Greenberg AH. Autocrine induction of tumor protease production and invasion by a metallothionein-regulated TGF-beta 1 (Ser223, 225). Embo J. 1992; 11:1599–1605. [PubMed: 1314170]

Sehgal I, Baley PA, Thompson TC. Transforming growth factor beta1 stimulates contrasting responses in metastatic versus primary mouse prostate cancer-derived cell lines in vitro. Cancer Res. 1996; 56:3359–3365. [PubMed: 8764134]

Shive MS, Anderson JM. Biodegradation and biocompatibility of PLA and PLGA microspheres. Adv Drug Deliv Rev. 1997; 28:5–24. [PubMed: 10837562]

Simionescu A, Philips K, Vyavahare N. Elastin-derived peptides and TGF-beta1 induce osteogenic responses in smooth muscle cells. Biochem Biophys Res Commun. 2005; 334:524–532. [PubMed: 16005428]

Simionescu A, Philips K, Vyavahare N. Elastin-derived peptides and TGF-beta 1 induce osteogenic responses in smooth muscle cells. Biochem Biophys Res Commun. 2005; 334:524–532. [PubMed: 16005428]

Sivaraman B, Ramamurthi A. Multifunctional nanoparticles for doxycycline delivery towards localized elastic matrix stabilization and regenerative repair. Acta Biomater. 2013; 9:6511–6525. [PubMed: 23376127]

Song CX, Labhasetwar V, Murphy H, Qu X, Humphrey WR, Shebuski RJ, Levy RJ. Formulation and characterization of biodegradable nanoparticles for intravascular local drug delivery. J Control Release. 1997; 43:197–212.

Song CX, Labhasetwar V, Murphy H, Qu X, Humphrey WR, Shebuski RJ, Levy RJ. Formulation and characterization of biodegradable nanoparticles for intravascular local drug delivery. J Control Release. 1997; 43:197–212.

Song J, Rolfe BE, Hayward IP, Campbell GR, Campbell JH. Effects of collagen gel configuration on behavior of vascular smooth muscle cells in vitro: association with vascular morphogenesis. In Vitro Cell Dev Biol Anim. 2000; 36:600–610. [PubMed: 11212145]

Soppimath KS, Aminabhavi TM, Kulkarni AR, Rudzinski WE. Biodegradable polymeric nanoparticles as drug delivery devices. Journal of Controlled Release. 2001; 70:1–20. [PubMed: 11166403]

Stechmiller J, Cowan L, Schultz G. The Role of Doxycycline as a Matrix Metalloproteinase Inhibitor for the Treatment of Chronic Wounds. Biol Res Nurs. 2010; 11:336–344. [PubMed: 20031955]

Stegemann JP, Nerem RM. Altered response of vascular smooth muscle cells to exogenous biochemical stimulation in two- and three-dimensional culture. Exp Cell Res. 2003; 283:146–155. [PubMed: 12581735]

Sunaric SM, Mitic SS, Miletic GZ, Pavlovic AN, Naskovic-Djokic D. Determination of doxycycline in pharmaceuticals based on its degradation by Cu(II)/H(2)O(2) reagent in aqueous solution. J Anal Chem. 2009; 64:231–237.

Sylvester A, Sivaraman B, Deb P, Ramamurthi A. Nanoparticles for localized delivery of hyaluronan oligomers towards regenerative repair of elastic matrix. Acta Biomaterialia. 2013; 9:9292–9302. [PubMed: 23917150]

Takahashi K, Ikura M, Habashita H, Nishizaki M, Sugiura T, Yamamoto S, Nakatani S, Ogawa K, Ohno H, Nakai H, Toda M. Novel matrix metalloproteinase inhibitors: generation of lead compounds by the in silico fragment-based approach. Bioorg Med Chem. 2005; 13:4527–4543. [PubMed: 15908222]

Tan Q, Tang H, Hu J, Hu Y, Zhou X, Tao Y, Wu Z. Controlled release of chitosan/heparin nanoparticle-delivered VEGF enhances regeneration of decellularized tissue-engineered scaffolds. Int J Nanomedicine. 2011; 6:929–942. [PubMed: 21720505]

Tewes F, Munnier E, Antoon B, Okassa LN, Cohen-Jonathan S, Marchais H, Douziech-Eyrolles L, Souce M, Dubois P, Chourpa I. Comparative study of doxorubicin-loaded poly(lactide-co-glycolide) nanoparticles prepared by single and double emulsion methods. Eur J Pharm Biopharm. 2007; 66:488–492. [PubMed: 17433641]

Tezvergil-Mutluay A, Agee KA, Uchiyama T, Imazato S, Mutluay MM, Cadenaro M, Breschi L, Nishitani Y, Tay FR, Pashley DH. The Inhibitory Effects of Quaternary Ammonium Methacrylates on Soluble and Matrix-bound MMPs. J Dent Res. 2011; 90:535–540. [PubMed: 21212315]

Thompson, RW.; Baxter, BT. MMP inhibition in abdominal aortic aneurysms - Rationale for a prospective randomized clinical trial. In: Greenwald, RA.; Zucker, S.; Golub, LM., editors. Inhibition of Matrix Metalloproteinases: Therapeutic Applications. Vol. 878. 1999. p. 159-178.

Uitto, VJ.; Firth, JD.; Nip, L.; Golub, LM. Doxycycline and chemically modified tetracyclines inhibit gelatinase A (MMP-2) gene expression in human skin keratinocytes. In: Greenwald, RA.; Golub, LM., editors. Inhibition of Matrix Metalloproteinases: Therapeutic Potential. Vol. 732. 1994. p. 140-151.

Venkataraman L, Ramamurthi A. Induced elastic matrix deposition within three-dimensional collagen scaffolds. Tissue Eng Part A. 2011; 17:2879–2889. [PubMed: 21702719]

Venkataraman L, Ramamurthi A. Induced elastin matrix generation within 3-dimensional collagen scaffolds. Tissue Eng Part A. 2011; 17:2879–2889. [PubMed: 21702719]

Visse R, Nagase H. Matrix metalloproteinases and tissue inhibitors of metalloproteinases - Structure, function, and biochemistry. Circ Res. 2003; 92:827–839. [PubMed: 12730128]

Wang X, Xu H, Zhao Y, Wang S, Abe H, Naito M, Liu Y, Wang G. Poly(lactide-co-glycolide) encapsulated hydroxyapatite microspheres for sustained release of doxycycline. Mater Sci Eng B. 2012; 177:367–372.

Welch DR, Fabra A, Nakajima M. Transforming growth factor beta stimulates mammary adenocarcinoma cell invasion and metastatic potential. Proc Natl Acad Sci U S A. 1990; 87:7678–7682. [PubMed: 2217201]

Wu XS. Synthesis, characterization, biodegradation, and drug delivery application of biodegradable lactic/glycolic acid polymers: Part III. Drug delivery application. Artif Cells Blood Substit Immobil Biotechnol. 2004; 32:575–591. [PubMed: 15974184]

Yamawaki-Ogata A, Hashizume R, Satake M, Kaneko H, Mizutani S, Moritan T, Ueda Y, Narita Y. A doxycycline loaded, controlled-release, biodegradable fiber for the treatment of aortic aneurysms. Biomaterials. 2010; 31:9554–9564. [PubMed: 20889203]

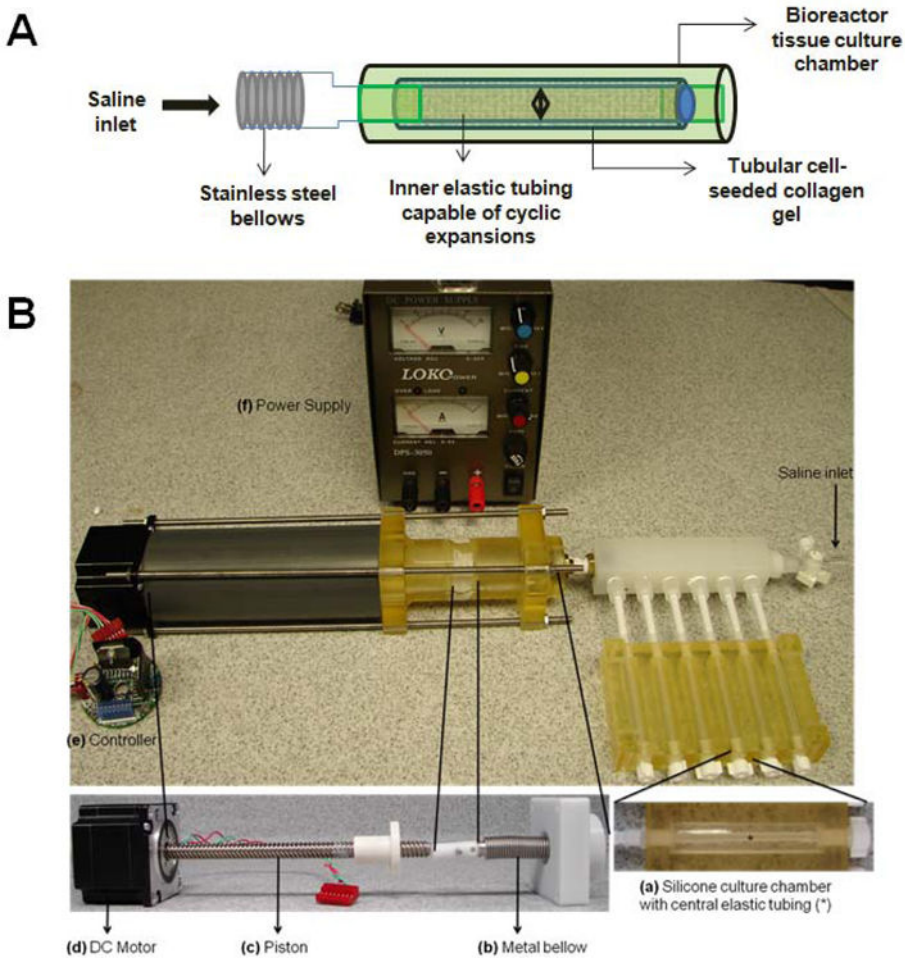

Figure 1.

(A) Schematic and (B) setup of multi-channel perfusion bioreactor capable of providing cyclic, circumferential stretch to tubular collagen gel constructs for 3-D dynamic culture. It consists of a cylindrical culture chamber (a), with centrally placed silicone tubing, around which the collagen gel constructs compacted. The silicone tubing was in turn connected to metallic bellows (b), forming a closed, airtight conduit into which a constant volume of water was maintained. The bioreactor worked on the principle that when the bellows contract and expand, the resultant displacement of water within the closed loop will proportionally expand or contract the silicone tube, and in turn the cell-seeded collagen gel construct around it. The contraction and expansion of the bellows were controlled by a stepper DC motor (d) and its controller (e), programmed to deliver the required 2.5 % strain at 1.5 Hz frequency via a piston (c).

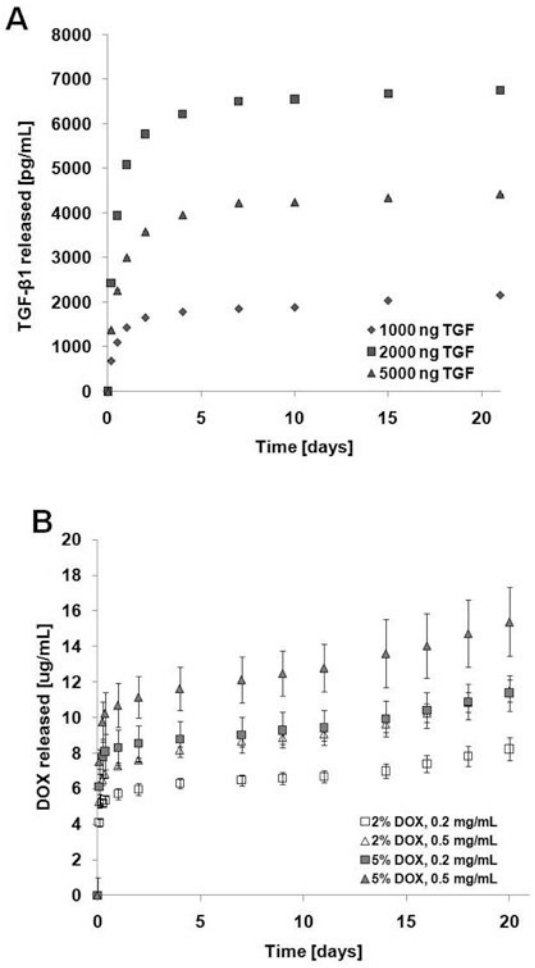

Figure 2.

In vitro release profiles for (A) TGF-β1 and (B) DOX from the PLGA NPs. TGF-β1 release studies were carried out at 10.0 mg/mL NP concentration for NPs loaded with 1000 ng, 2000 ng and 5000 ng TGF-β1. Two different DOX loadings (2% and 5% w:w DOX:PLGA ratios) at three NP concentrations (0.2, 0.5 and 1.0 mg/mL) were utilized for DOX release curves. (n = 3 per group; mean ± SD).

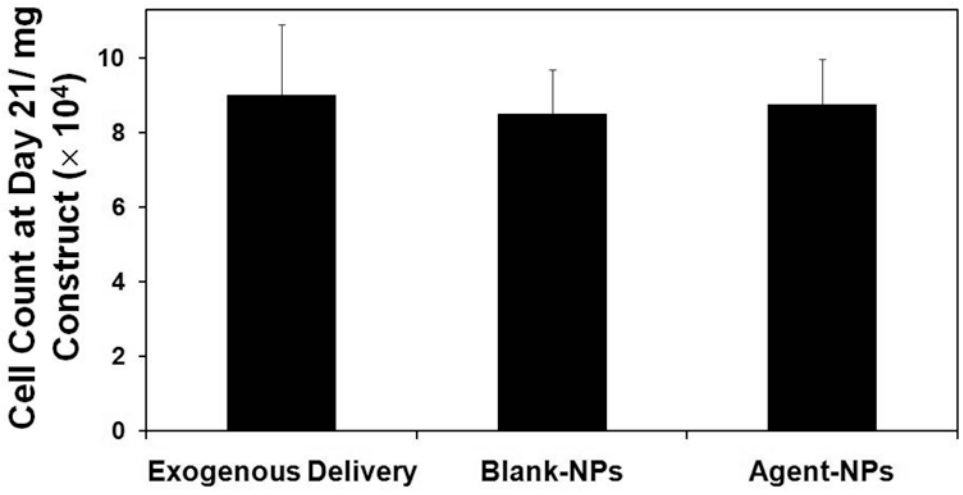

Figure 3.

Proliferation of human aortic smooth muscle cells (HASMCs) in response to the addition of blanks NPs (0.5 mg/mL) and agent-loaded NPs (0.2 mg/mL of 2% DOX-NPs and 0.3 mg/mL of 2000 ng TGF-β1 loaded NPs), compared to exogenous delivery (EDC) of TGF-β1 (0.2 ng/mL) and DOX (11.4 μg/mL). The cell number was calculated based on an estimate of 6 pg of DNA per cell, via a DNA assay at 21 days post-seeding, and normalized to mg tissue weights for comparison (mean ± SD; $n = 5$ per case).

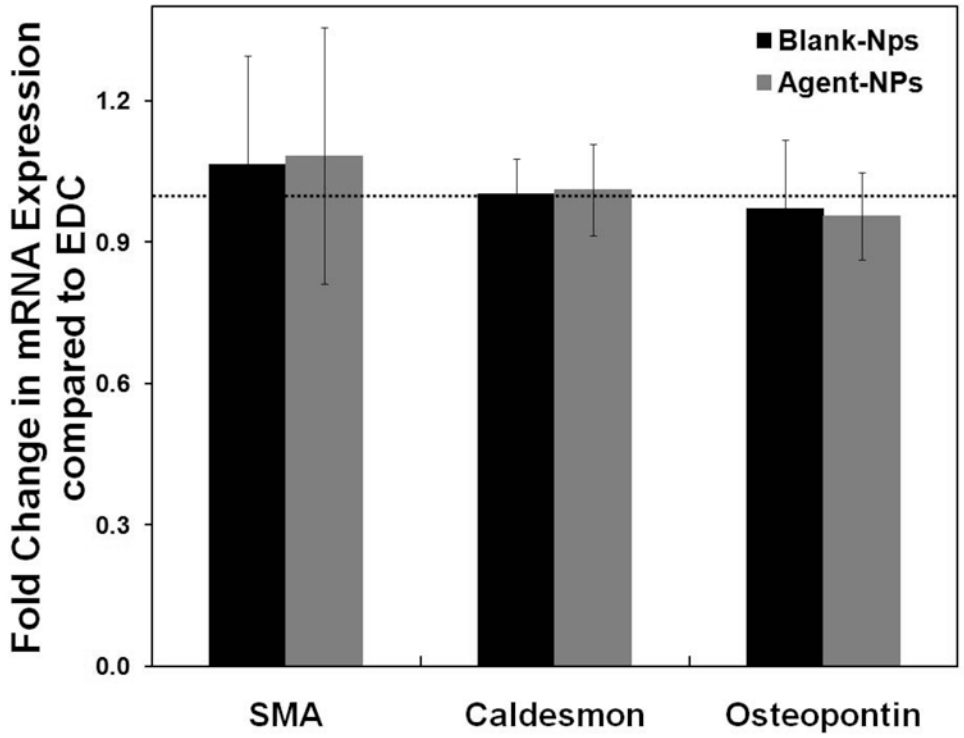

Figure 4.

Effects of NP addition on phenotypic response of HASMCs, as analyzed via PCR. Fold-change in mRNA expression of α-smooth muscle active (SMA), caldesmon and osteopontin, compared to EDC controls ($n = 5$ per treatment condition). The mRNA expression levels for the different phenotypic markers for the EDC condition was set to unity to determine the fold change in their expression for the blank- (BNP) and agent-loaded NP (ANP) treated test cases.

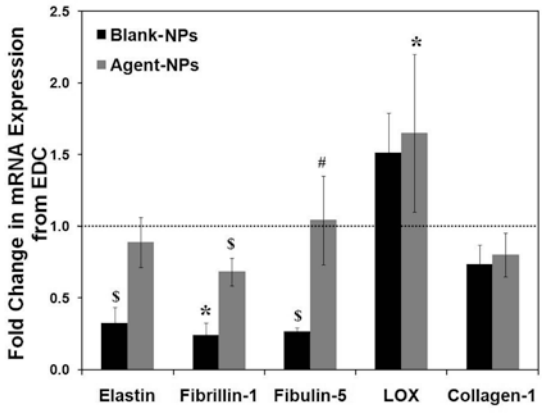

Figure 5A

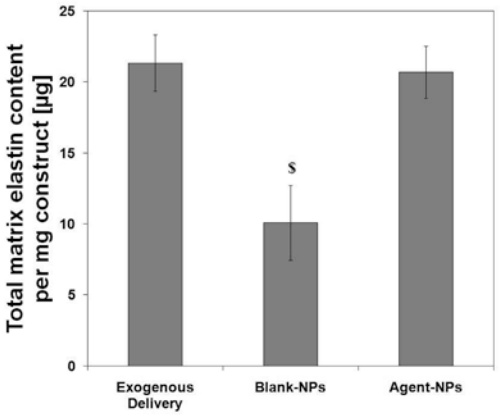

Figure 5B

Figure 5.

Effects of NPs on expression of elastic matrix-associated proteins. (A) Fold-change in mRNA expression of elastin, fibrillin-1, fibulin-5, lysyl oxidase (LOX) and collagen-1 compared to EDC controls ($n = 5$ per treatment condition, * denotes $p < 0.05$ compared to EDC, # denotes $p < 0.05$ compared to BNP, $ denotes $p < 0.05$ compared to every treatment condition). The mRNA expression levels for the different phenotypic markers for the EDC condition was set to unity to determine the fold change in their expression for the blank- (BNP) and agent-loaded NP (ANP) treated test cases. (B) Comparison of total matrix elastin deposition by HASMCs for the different agent delivery modes. The elastic matrix content was normalized to the construct weights for comparison ($ denotes $p < 0.05$ compared to every treatment condition).

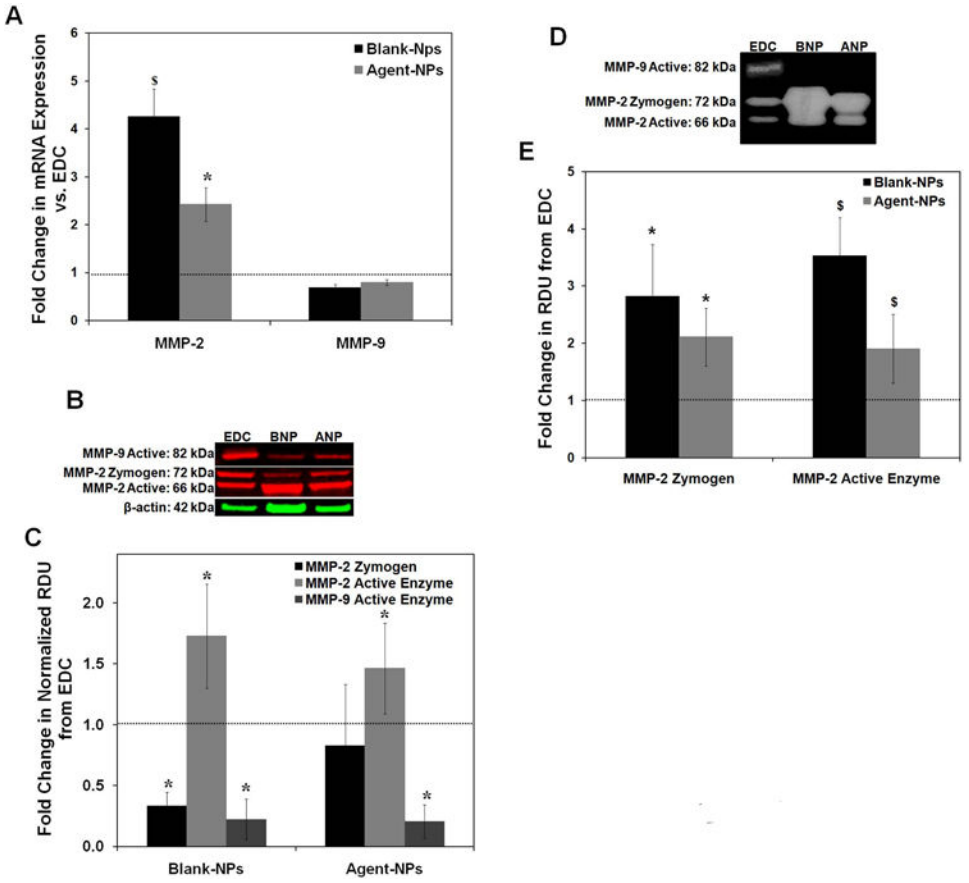

Figure 6.

Effect of NPs on MMP expression and activity by HASMCs. (A) Fold-change in mRNA expression of MMP-2 and -9 compared to exogenous delivery control (EDC). ($n = 5$ per treatment condition, * denotes $p < 0.05$ compared to EDC, $ denotes $p < 0.05$ compared to every treatment condition). (B) Representative western blot image illustrating the synthesis of MMP-2 and -9 by HASMCs within the constructs, with β-actin (loading control). (C) Fold-change in expression of MMP-2 zymogen, and active forms of MMP-2 and -9 compared to exogenous delivery control (EDC; set to unity). ($n = 3$ per treatment condition; * denotes $p < 0.05$ compared to EDC). (D) Representative gel zymograms showing the active and zymogen forms of MMP-2 and active form of MMP-9. (E) Fold-change in zymogen and active forms of MMP-2 compared to exogenous delivery control (EDC; set to unity) ($n = 3$ per treatment condition; * denotes $p < 0.05$ compared to EDC, $ denotes $p < 0.05$ compared to every treatment condition).

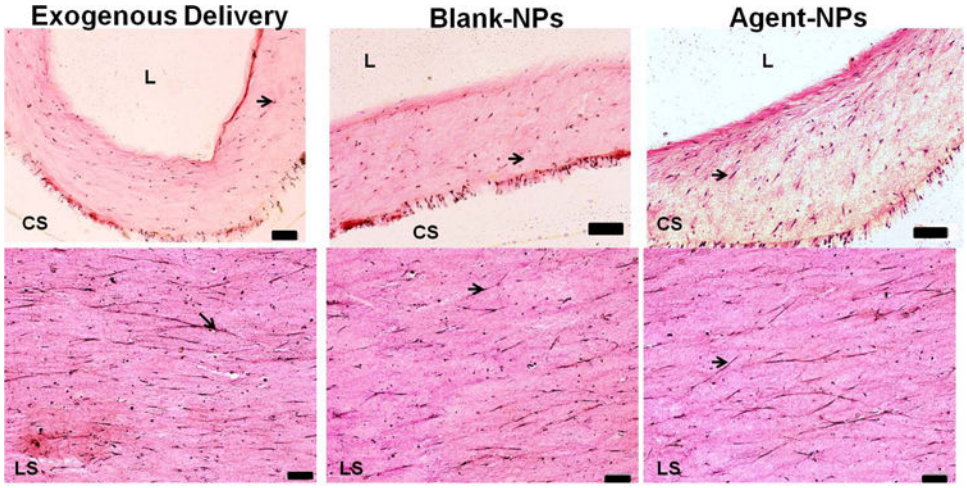

Figure 7.

Elastic staining of 30 μm thick cross- (CS; upper panel) and longitudinal sections (LS; lower panel) of collagen constructs (stained pink) after 21 days of treatment. Orientation of cells and elastic fibers (stained purple/black, indicated by arrows) were seen in the longitudinal direction. (Scale bars for upper panel are equivalent to 100 μm; scale bars for lower panel equivalent to 500 μm)

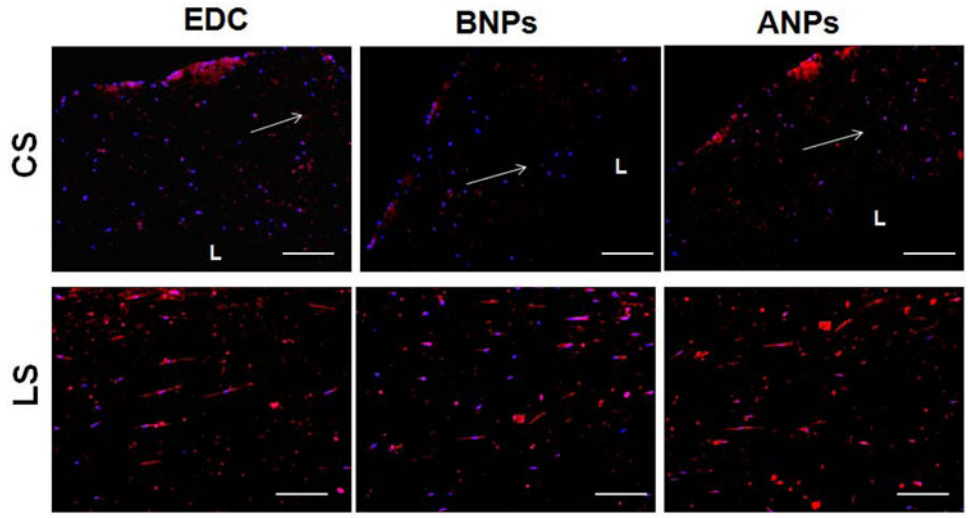

Figure 8.

Representative images of 10 μm thick sections of collagen constructs labeled for immunofluorescent detection of elastin, following 21 days of treatment. Elastin (red) was detected in (upper panel) cross- and (lower panel) longitudinal sections of the constructs. Nuclei were stained with DAPI (middle panels). White arrows indicate longitudinal direction of constructs. L = lumen. Magnification = 10 ×. Scale bar equivalent to 200 μm.

Table 1

Size and surface charge of TGF-β1 encapsulated PLGA NPs, formulated with 0.25 % w/v PVA as the surfactant/stabilizer. (n = 6, mean ± S.D).

	TGF-β1 loading [ng]		
	1000	**2000**	**5000**
Size [nm]	295.7 ± 5.1	351.6 ± 9.8	347.3 ± 40.3
ζ-potential [mV]	-28.1 ± 2.0	-25.5 ± 2.7	-25.9 ± 3.0
Encapsulation efficiency [%]	85.7 ± 1.2	73.7 ± 14.6	91.4 ± 3.0

Table 2

Size and surface charge of DOX-encapsulated PLGA NPs, formulated with 0.25 % w/v PVA as the surfactant/stabilizer. (n = 6, mean ± S.D).

	Blank NPs	DOX loading [%; w/w ratio to PLGA]	
	Agent-free	2	5
Size [nm]	386.8 ± 46.5	343.8 ± 5.3	342.3 ± 1.4
ζ-potential [mV]	-30.3 ± 2.3	-28.2 ± 1.0	-31.6 ± 1.0
Encapsulation efficiency [%]	N/A	58.3 ± 0.5	57.9 ± 0.9

Table 3

Forward and reverse primer sequences of genes designed using Perl Primer.

Gene	Primer Sequence (5′-3′)		Size (bp)
Fibrillin- 1 (*FBLN1*)	Forward	GCTCCAGATCCATACAACAC	145
	Reverse	ACACCTTCCTCCATTGAGAC	
Collagen-1 (*COL1A1*)	Forward	AAGGGACACAGAGGTTTCAG	189
	Reverse	TAGCACCATCATTTCCACGA	
Caldesmon (*CALD1*)	Forward	CCCAAACCTTCTGACTTGAG	162
	Reverse	CGAATTAGCCCTCTACAACTG	
Osteopontin-1 (*OPN1*)	Forward	TGTGCCATACCAGTTAAACAG	147
	Reverse	ACTTACTTGGAAGGGTCTGTG	